7. Kurata Y, Fujimura K, Kuwana M, Tomiyama Y, Murata M. Epidemiology of primary immune thrombocytopenia in children and adults in Japan: a population-based study and literature review. Int J Hematol. 2011;93:329–35.
8. Provan D, Stasi R, Newland AC, Blanchette VS, Bolton-Maggs P, Bussel JB, et al. International consensus report on the investigation and management of primary immune thrombocytopenia. Blood. 2009;115:168–86.
9. Neunert C, Lim W, Crowther M, Cohen A, Solberg L Jr. The American Society of Hematology 2011 evidence-based practice guideline for immune thrombocytopenia. Blood. 2011;117: 4190–207.
10. Arnold DM, Bernotas A, Nazi I, Stasi R, Kuwana M, Liu Y, et al. Platelet count response to *H. pylori* treatment in patients with immune thrombocytopenic purpura with and without *H. pylori* infection: a systematic review. Haematologica. 2009;94:850–6.
11. Arnold DM, Stasi R. Does *Helicobacter pylori* eradication therapy result in a platelet count improvement in adults with immune thrombocytopenic purpura regardless of *H pylori* infection? ASH evidence-based review. Hematology Am Soc Hematol Educ Program. 2008;2008:31–2.
12. Kuwana M, Ikeda Y. *Helicobacter pylori* and immune thrombocytopenic purpura: unsolved questions and controversies. Int J Hematol. 2006;84:309–15.
13. Suzuki T, Matsushima M, Masui A, Watanabe K, Takagi A, Ogawa Y, et al. Effect of *Helicobacter pylori* eradication in patients with chronic idiopathic thrombocytopenic purpura-a randomized controlled trial. Am J Gastroenterol. 2005;100: 1265–70.
14. Tsumoto C, Tominaga K, Okazaki H, Tanigawa T, Yamagami H, Watanabe K, et al. Long-term efficacy of *Helicobacter pylori* eradication in patients with idiopathic thrombocytopenic purpura: 7-year follow-up prospective study. Ann Hematol. 2009;88:789–93.
15. McMillan R. Therapy for adults with refractory chronic immune thrombocytopenic purpura. Ann Intern Med. 1997;126:307–14.
16. Stasi R, Provan D. Management of immune thrombocytopenic purpura in adults. Mayo Clin Proc. 2004;79:504–22.
17. Nomura S, Dan K, Hotta T, Fujimura K, Ikeda Y. Effects of pegylated recombinant human megakaryocyte growth and development factor in patients with idiopathic thrombocytopenic purpura. Blood. 2002;100:728–30.
18. Rank A, Weigert O, Ostermann H. Management of chronic immune thrombocytopenic purpura: targeting insufficient megakaryopoiesis as a novel therapeutic principle. Biologics. 2010;4:139–45.
19. Nplate (romiplostim), European Public Assessment Report summary. 2009.
20. Nplate™ (romiplostim) Prescribing Information. Amgen, Inc., Thousand Oaks, CA. 2011.
21. Nplate™ (romiplostim) Prescribing Information. European Medicines Agency. Amgen, Inc., Thousand Oaks, CA. 2011.
22. Romiplate prescribing information. 2011; http://www.mhlw.go.jp/stf/shingi/2r985200000136yg-att/2r9852000001372i.pdf.
23. Burroughs VJ, Maxey RW, Levy RA. Racial and ethnic differences in response to medicines: towards individualized pharmaceutical treatment. J Natl Med Assoc. 2002;94:1–26.
24. Matthews HW. Racial, ethnic and gender differences in response to medicines. Drug Metabol Drug Interact. 1995;12:77–91.
25. Kumagai Y, Fujita T, Ozaki M, Sahashi K, Ohkura M, Ohtsu T, et al. Pharmacodynamics and pharmacokinetics of AMG 531, a thrombopoiesis-stimulating peptibody, in healthy Japanese subjects: a randomized, placebo-controlled study. J Clin Pharmacol. 2007;47:1489–97.
26. Shirasugi Y, Ando K, Hashino S, Nagasawa T, Kurata Y, Kishimoto Y, et al. A phase II, open-label, sequential-cohort, dose-escalation study of romiplostim in Japanese patients with chronic immune thrombocytopenic purpura. Int J Hematol. 2009;90:157–65.
27. Shirasugi Y, Ando K, Miyazaki K, Tomiyama Y, Okamoto S, Kurokawa M, et al. Romiplostim for the treatment of chronic immune thrombocytopenia in adult Japanese patients: a double-blind, randomized Phase III clinical trial. Int J Hematol. 2011;94: 71–80.
28. Kuter DJ, Bussel JB, Lyons RM, Pullarkat V, Gernsheimer TB, Senecal FM, et al. Efficacy of romiplostim in patients with chronic immune thrombocytopenic purpura: a double-blind randomised controlled trial. Lancet. 2008;371:395–403.
29. Gupta S, Indelicato SR, Jethwa V, Kawabata T, Kelley M, Mire-Sluis AR, et al. Recommendations for the design, optimization, and qualification of cell-based assays used for the detection of neutralizing antibody responses elicited to biological therapeutics. J Immunol Methods. 2007;321:1–18.
30. Mason S, La S, Mytych D, Swanson SJ, Ferbas J. Validation of the BIACORE 3000 platform for detection of antibodies against erythropoietic agents in human serum samples. Curr Med Res Opin. 2003;19:651–9.
31. Mire-Sluis AR, Barrett YC, Devanarayan V, Koren E, Liu H, Maia M, et al. Recommendations for the design and optimization of immunoassays used in the detection of host antibodies against biotechnology products. J Immunol Methods. 2004;289:1–16.
32. Kuter DJ, Bussel JB, Newland A, Wasser JS, Lyons RM, George JN, et al. Long-term efficacy and safety of romiplostim treatment of adult patients with chronic immune thrombocytopenia (ITP): final report from an open-label extension study. ASH Annu Meet Abstr. 2010;116:68.
33. Bussel JB, Kuter DJ, Pullarkat V, Lyons RM, Guo M, Nichol JL. Safety and efficacy of long-term treatment with romiplostim in thrombocytopenic patients with chronic ITP. Blood. 2009;113: 161–71.
34. Kuter DJ, Rummel M, Boccia R, Macik BG, Pabinger I, Selleslag D, et al. Romiplostim or standard of care in patients with immune thrombocytopenia. N Engl J Med. 2010;363:1889–99.

Leukemia (2012) 26, 303–311

www.nature.com/leu

ORIGINAL ARTICLE

C-terminal mutation of *RUNX1* attenuates the DNA-damage repair response in hematopoietic stem cells

Y Satoh[1], I Matsumura[2], H Tanaka[2], H Harada[3], Y Harada[4], K Matsui[1], M Shibata[1], M Mizuki[1] and Y Kanakura[1]

[1]*Department of Hematology and Oncology, Osaka University Graduate School of Medicine, Suita, Japan;* [2]*Department of Internal Medicine, Division of Hematology, Faculty of Medicine, Kinki University, Osaka-sayama, Japan;* [3]*Department of Hematology and Oncology, Research Institute for Radiation Biology and Medicine, Hiroshima University, Hiroshima, Japan and* [4]*International Radiation Information Center, Research Institute for Radiation Biology and Medicine, Hiroshima University, Hiroshima, Japan*

Loss-of-function mutations of *RUNX1* have been found in acute myeloid leukemia (AML) and myelodysplastic syndromes (MDSs). Although several reports have suggested roles for RUNX1 as a tumor suppressor, its precise function remains unknown. Because gene alterations of *RUNX1* by themselves do not lead to the development of leukemia in mouse models, additional mutation(s) would be required for leukemia development. Here, we report that the C-terminal deletion mutant of *RUNX1*, RUNX1dC, attenuates DNA-damage repair responses in hematopoietic stem/progenitor cells. γH2AX foci, which indicate the presence of DNA double-strand breaks, were more abundantly accumulated in RUNX1dC-transduced lineage$^-$ Sca1$^+$c-kit$^+$ (LSK) cells than in mock-transduced LSK cells both in a steady state and after γ-ray treatment. Expression profiling by real-time -PCR array revealed RUNX1dC represses the expression of *Gadd45a*, a sensor of DNA stress. Furthermore, bone marrow cells from MDS/AML patients harboring the *RUNX1*-C-terminal mutation showed significantly lower levels of *GADD45A* expression compared with those from MDS/AML patients with wild-type *RUNX1*. As for this mechanism, we found that RUNX1 directly regulates the transcription of *GADD45A* and that RUNX1 and p53 synergistically activate the *GADD45A* transcription. Together, these results suggest Gadd45a dysfunction due to *RUNX1* mutations can cause additional mutation(s) required for multi-step leukemogenesis.

Leukemia (2012) **26,** 303–311; doi:10.1038/leu.2011.202; published online 12 August 2011
Keywords: RUNX1; DNA damage; GADD45A; acute myeloid leukemia; myelodysplastic syndromes

Introduction

Myelodysplastic syndromes (MDSs) are clonal hematological disorders derived from gene alterations at the level of hematopoietic stem cells, which are characterized by ineffective hematopoiesis, dysplastic morphology of blood cells and a high possibility of transition to acute myeloid leukemia (AML). A number of genetic or epigenetic alterations involved in the pathogenesis of MDS have been identified: activating point mutations of signaling molecules such as N-RAS and FLT3;[1] deletion, point mutations and/or silencing of cell cycle inhibitory molecules such as p15 and p53;[2,3] deletion, point mutations and generation of chimeric genes from transcriptional factors such as EVI-1 and RUNX1;[4,5] and point mutations of nuclear proteins such as nucleophosmin and TET2.[6,7] Among these changes, point mutations of *RUNX1* have been detected in about 10–20% of patients classified as MDS/AML (high-risk MDS and AML following MDS).[5] The transcription factor RUNX1 and its heterodimeric partner core-binding factor (CBF)β (also known as phosphatidylethanolamine-binding protein2β) comprise CBFs. CBFs are the most frequent targets of gene rearrangement and mutation in human leukemias; leukemias harboring mutations in either subunit of a CBF are commonly called CBF leukemias.[8] Recently, Tang *et al.*[9] reported *RUNX1* mutations were detected in 13.2% of 470 adult patients with *de novo* AML. In addition, hereditary loss-of-function mutations of *RUNX1* cause familial platelet disorder with predisposition to AML, which is characterized by decreased platelet count and propensity to develop AML.[10] These findings suggest RUNX1 works as a tumor suppressor and impaired RUNX1 function promotes leukemia development. Nonetheless, *RUNX1* deletion or dominant-negative inhibition of RUNX1 by itself is not sufficient for leukemia development in several mouse models,[11,12] indicating that additional cooperating events are required. However, the mechanisms by which impaired RUNX1 functions lead to subsequent genetic alterations are not fully understood.

Cells in the human body are always exposed to DNA stresses, which induce damages to chromosomal DNA.[13] Physiological stresses such as hydrolytic reactions, non-enzymatic methylations and oxygen radicals generate DNA-base lesions.[14] Environmental agents such as ultraviolet (UV), ionizing radiation and a lot of genotoxic chemicals also induce DNA damages including single- and double-strand breaks (DSBs). These DNA lesions are repaired through damage-specific repair pathways. However, if these lesions are left unrepaired, these cells alone and/or in combination with additional mutations would have a higher risk of tumor development.[15] In a previous study, it was reported that *Runx1*-deficient mice had an increased incidence of hematological malignancy compared with wild-type (WT) mice after treatment with the mutagen, *N*-ethyl-*N*-nitrosourea.[16]

We speculated RUNX1 might have a role in the DNA-damage repair (DDR) response. Here, we show that a C-terminal deletion mutant of *RUNX1*, RUNX1dC, enhances DNA-damage accumulation in hematopoietic stem cell-enriched lineage$^-$Sca1$^+$c-kit$^+$ (LSK) cells. Furthermore, we found RUNX1dC attenuates the DDR response after exposure to DNA-damage agents. As for this mechanism, we found that RUNX1dC suppresses the transcription of a sensor of DNA stress, *Gadd45a*.[17] Moreover, bone marrow (BM) cells from MDS/AML patients harboring a *RUNX1*-C-terminal mutation showed significantly lower *GADD45A* expression than those from MDS/AML patients with WT *RUNX1*. These results suggest RUNX1

Correspondence: Dr Y Satoh, Department of Hematology and Oncology, Osaka University Graduate School of Medicine, C9, 2-2, Yamada-oka, Suita, Osaka, 565-0871, Japan.
E-mail: ysatoh@bldon.med.osaka-u.ac.jp
Received 26 August 2010; revised 31 May 2011; accepted 30 June 2011; published online 12 August 2011

regulates *Gadd45a* transcription and impaired RUNX1 function can cause additional mutation(s) required for multi-step leukemogenesis.

Materials and methods

Real-time (RT)-PCR array

Total cellular RNA was extracted from 4×10^6 cells using the RNeasy Mini Kit (Qiagen, Tokyo, Japan). A total of 4 μg of RNA was reverse-transcribed into cDNA using the RT^2 First Strand Kit (SABiosciences, Frederick, MD, USA) and subjected to RT-PCR array analysis (RT^2Profiler PCR Array: Mouse DNA Damage Signaling, SABiosciences). Gene expression profiles of 32D-neo and 32D-RUNX1dC cells were analyzed by the ΔΔCt method.

Colony-forming assay

32D-neo and 32D-RUNX1dC cells (1×10^5 cells) were suspended in 500 μl of phosphate buffered saline and exposed to UV-B (800 or 1600 J/m^2). Then, cells were washed twice with PBS containing 2% FBS, plated into dishes (1×10^3 cells/dish) and cultured in the methylcellulose media M3231 (Stem Cell Technologies, Vancouver, British Colombia, Canada) containing mouse interleukin-3 (mIL-3). Colony numbers were counted after 7 days of culture. Also, retrovirus-transfected LSK cells were exposed to UV-B (2400 J/m^2), plated into dishes (2×10^3 cells/dish) and cultured in methylcellulose media M3434 (Stem Cell Technologies) containing mSCF, mIL-3, human IL-6 (hIL-6) and human erythropoietin. Colony numbers were counted after 10 days. All experiments were carried out in triplicate. DNA repair activities of the test cells are represented relative to those of untreated cells.

Quantitative PCR assays for the expression of GADD45A in MDS/AML patients

Total cellular RNA was extracted from BM mononuclear cells of 23 MDS/AML patients, 5 healthy donors and 5 non-Hodgkin

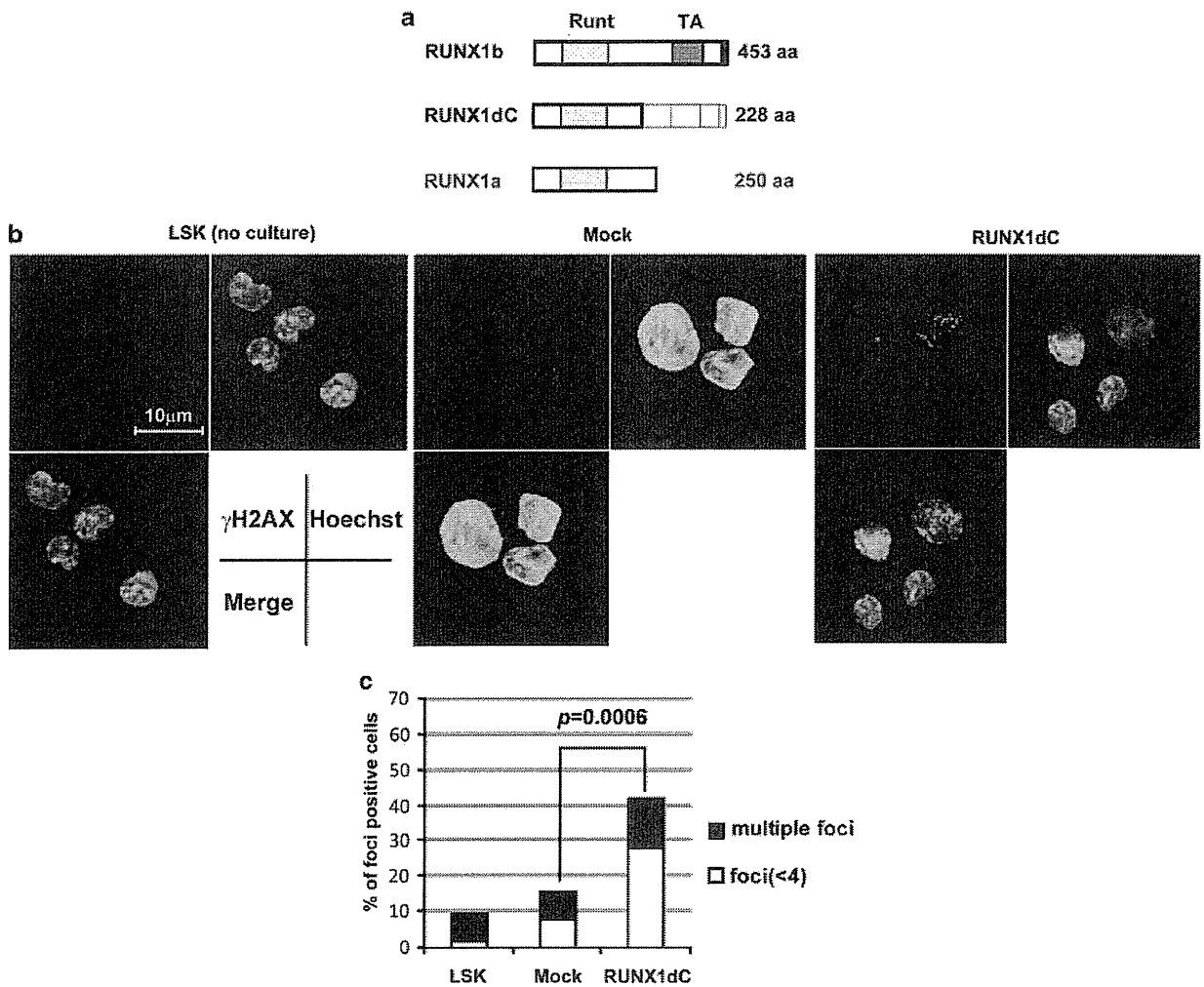

Figure 1 RUNX1dC induces DNA-damage accumulation in LSK cells. (**a**) Structures of WT RUNX1 (RUNX1b), RUNX1dC and RUNX1a. RUNX1dC lacks 225 C-terminal amino acids because of the insertion of ACCGT at 669–670 bp, which causes a frameshift mutation. (**b**) Accumulations of DSBs in Mock- and RUNX1dC-transduced LSK cells were detected by γH2AX antibody (2 days after gene transduction). LSK refers to LSK cells just after FACS sorting. Hoechst refers to Hoechst 33342. The scale bar (10 μm) applies to all images. (**c**) The percentage of γH2AX foci-positive cells in Mock- and RUNX1dC-transduced LSK cells. Results shown are the average of three experiments. Open square indicates % of γH2AX foci-positive cells (with fewer than four foci per cell), and closed square indicates % of multiple foci-positive cells (four or more foci per cell).

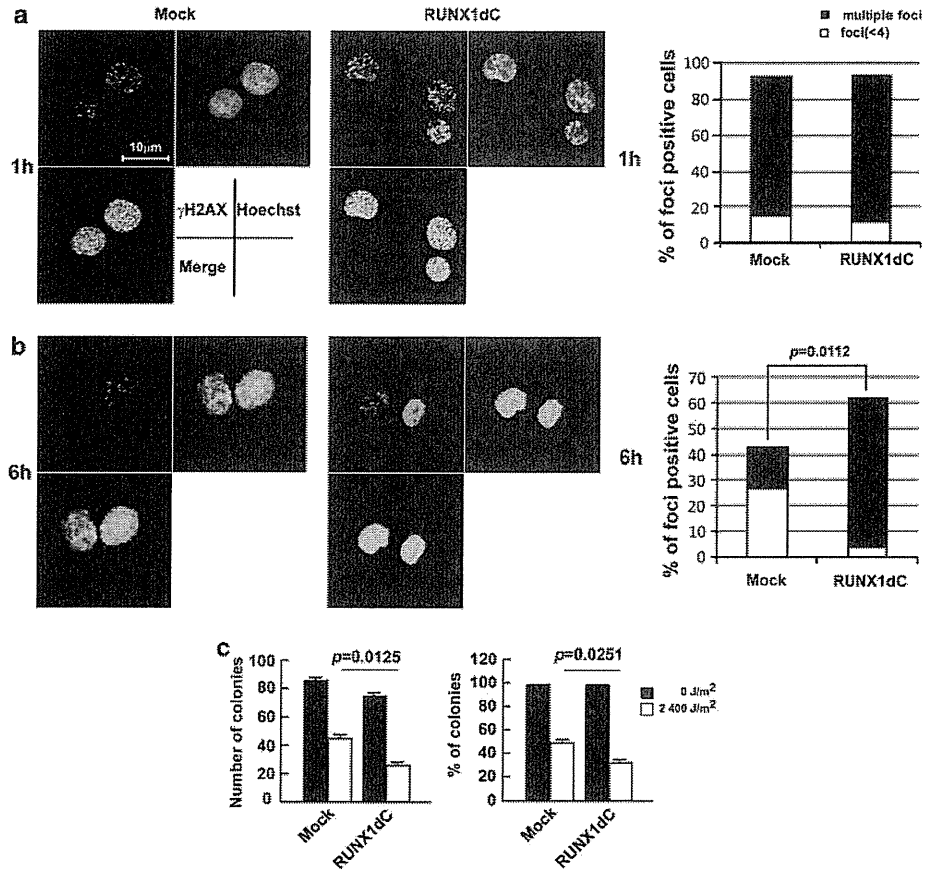

Figure 2 RUNX1dC-transduced cells attenuate the DDR response to double-strand breaks in LSK cells. (**a**) Accumulations of γH2AX foci in Mock- and RUNX1dC-transduced LSK cells 1 h after γ-ray treatment (left panel). Hoechst refers to Hoechst 33342. The scale bar (10 μm) applies to all images. The percentage of γH2AX foci-positive cells in Mock- and RUNX1dC-transduced LSK cells are shown (right panel). Results are the average of three experiments. Open square indicates % of γH2AX foci-positive cells (with fewer than four foci per cell), and closed square indicates % of multiple foci-positive cells (four or more foci per cell). (**b**) Accumulations of γH2AX foci in Mock- and RUNX1dC-transduced LSK cells 6 h after γ-ray treatment (left panel). The percentage of γH2AX foci-positive cells in Mock- and RUNX1dC-transduced LSK cells 6 h after γ-ray treatment are shown (right panel). (**c**) Colony-forming ability of Mock- and RUNX1dC-transduced LSK cells after UV-B treatment. Each bar shows absolute colony numbers (left panel) or the % of colonies relative to those of non-treated cells (right panel). Data are means ± s.e.m. of triplicate experiments.

lymphoma patients, who did not have BM involvement of the disease, as controls. All of the MDS/AML patients were diagnosed at Hiroshima University Hospital and its affiliated hospitals between 2000 and 2005. Diagnosis was made based on morphologic and immunophenotypic studies according to the French-American-British classification.[18] Clinical characteristics of MDS/AML patients are shown in Supplementary Table 2.[19] This project was approved by the Institutional Review Board at Hiroshima University, and BM samples were taken after obtaining informed consent. Probes and primers used in the quantitative PCR assay are listed in the Supplementary Methods.

Statistical analysis

All values are expressed as means ± s.e.m. We performed statistical analysis using Student's *t*-test. Values were considered statistically significant at $P<0.05$.

Results

RUNX1dC induces DNA-damage accumulation in LSK cells

DNA-damage accumulation and its repair pathways have important roles in tumor development.[13] Thus, we first evaluated DNA-damage accumulation in a C-terminal truncated RUNX1 mutant-transduced LSK cells. In this study, we utilized the RUNX1dC, which lacks 225 amino acids covering both transactivating and transrepressing domains of WT RUNX1 (Figure 1a). This mutant was originally identified in a patient with MDS, and we and others previously showed it functions as a dominant-negative mutant over WT RUNX1 (RUNX1b) by inhibiting its DNA-binding activity.[20,21] RUNX1dC resembles in size an isoform of RUNX1, RUNX1a, (Figure 1a), which also has an inhibitory effect against RUNX1b.[22] Two days after gene transduction, we evaluated accumulations of DSBs using an antibody recognizing the phosphorylated histone variant H2AX at serine 139 (γH2AX).[23] As shown in Figures 1b and c, more DSBs were detected in RUNX1dC-transduced LSK cells than in Mock-transduced LSK cells (42% foci-positive cells in RUNX1dC-transduced cells vs 15% foci-positive cells in Mock-transduced cells, $P=0.0006$).

RUNX1dC transduction results in the attenuation of the DDR response to DSBs in LSK cells

We next examined the DDR response in RUNX1dC-transduced LSK cells after exposure to environmental stressors. γH2AX foci, which indicate the immediate chromatin modification in

response to the formation of DSBs, reached a peak 30–60 min after irradiation (Figure 2a). Thereafter, the number of foci decreased with a half-life of several hours due to the DNA-repair response to DSBs.[24] Therefore, sustained accumulation of γH2AX foci indicates attenuation of the DDR response to DSBs. A total of 6 h after γ-ray treatment, RUNX1dC-transduced cells showed significantly higher accumulation of γH2AX foci than Mock-transduced LSK cells ($P=0.0112$; Figure 2b). Moreover, although the percentage of multiple foci-positive cells carrying more severe accumulations of DSBs was only 37.6% among γH2AX-positive cells in Mock transduction, most (93.5%) γH2AX-positive cells had multiple foci in RUNX1dC-transduced LSK cells (Figure 2b right panel). In addition, we analyzed the colony-forming ability of Mock- or RUNX1dC-transduced LSK cells after treatment with UV-B. In this assay, the DDR response of tested cells can be measured by relative colony numbers because only cells that recovered from DNA damage can make colonies.[25] At steady state, there was no significant difference in colony-forming ability between Mock- and RUNX1dC-transduced LSK cells (Figure 2c left panel). On the other hand, analyses of relative colony numbers revealed RUNX1dC-transduced LSK cells showed significantly lower colony-forming ability than Mock-transduced LSK cells after UV-B exposure (32.2% in RUNX1dC-transduced LSK vs 48.8% in Mock-transduced LSK, $P=0.0251$; Figure 2c right panel).

RUNX1dC suppresses Gadd45a expression in LSK cells

As DSBs were more prominent in RUNX1dC-transduced LSK cells than in Mock-transduced LSK cells, we speculated that the defect in the DDR response gene may be a cause of enhanced DNA-damage accumulation in RUNX1dC-transduced LSK cells. Therefore, we next examined whether RUNX1dC alters expressions of DNA-damage signaling molecules. We prepared 32Dcl3 cells expressing RUNX1dC and confirmed expression by immunoblot (Supplementary Figure 1). We profiled the expression of 84 genes involved in DNA-damage signaling by RT-PCR array using this subclone. Before performing the RT-PCR array experiment, we confirmed 32D-RUNX1dC showed significantly lower colony-forming ability than 32D-neo cells after UV-B exposure, just like RUNX1dC-transduced LSK cells (at 1600 J/m^2: 38.2% in 32D-RUNX1dC vs 67.2% in 32D-neo, $P<0.0234$; Figure 3a right panel). Furthermore, we evaluated the accumulation of cyclobutane pyrimidine dimers, which are major products of DNA damage induced by UV-B, in 32D-neo and 32D-RUNX1dC cells.[26] There was no distinct difference in cyclobutane pyrimidine dimer accumulation between 32D-neo and 32D-RUNX1dC cells before UV-B treatment (Figure 3b). Although 1 h after UV-B treatment the levels of cyclobutane pyrimidine dimer accumulation were the same in 32D-neo and 32D-RUNX1dC cells, the removal of cyclobutane pyrimidine dimer was significantly impaired in 32D-RUNX1dC cells compared with 32D-neo (Figure 3b). In addition, as with RUNX1dC-transduced LSK cells, 32D-RUNX1dC cells showed sustained accumulation of γH2AX foci after γ-ray irradiation (Figure 4b). After correction using five housekeeping genes (*Gusb*, *Hprt1*, *Hsp90ab1*, *Gapdh* and *Actb*), we obtained four candidate genes, in which expression was repressed in 32D-RUNX1dC cells compared with 32D-neo cells with a fold-difference cutoff of <0.5 (Figure 3c and Supplementary Table 1). Among these candidate genes, the expression of *Gadd45a* was particularly decreased in 32D-RUNX1dC cells compared with 32D-neo cells (Figure 3c and Supplementary Figure 2a). Quantitative RT-PCR using 32D-RUNX1dC and 32D-neo cells confirmed the expression of *Gadd45a* was

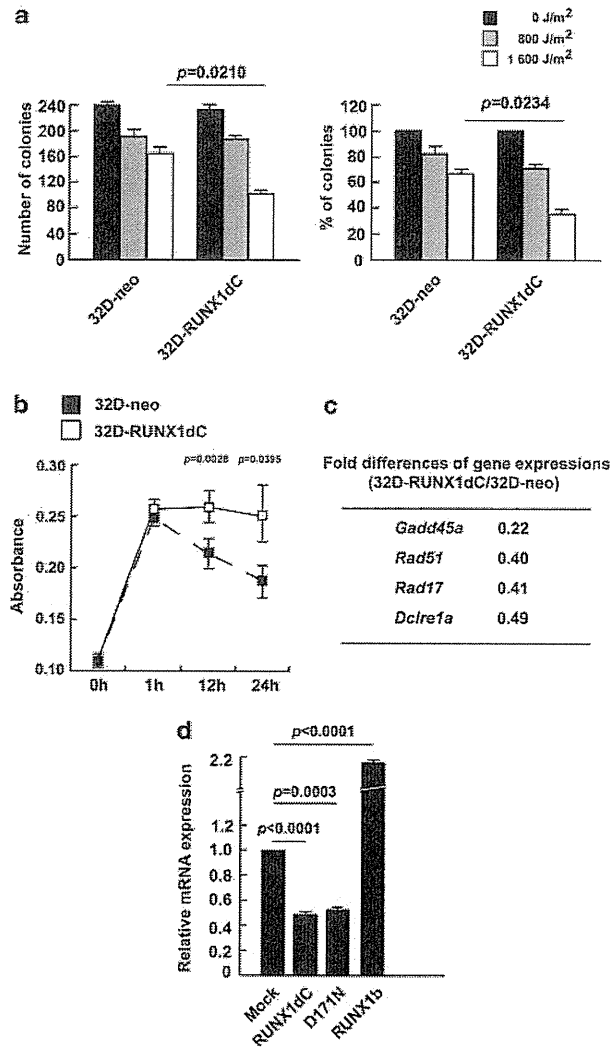

Figure 3 RUNX1dC suppresses *Gadd45a* expression in LSK cells. (**a**) Colony-forming assays for 32D-neo and 32D-RUNX1dC cells after treatment with UV-B. Test cells (1×10^3) were plated onto methylcellulose medium and cultured with IL-3. Each bar shows absolute colony numbers (left panel) or the % of colonies relative to that of non-treated cells (right panel). Data are means ± s.e.m. of triplicate experiments. (**b**) Determination of UV-B induced DNA damage by enzyme linked immunosorbant assay using anti-cyclobutane pyrimidine dimers antibody. Data are means ± s.e.m. of quadruplicate experiments. (**c**) Expression profiling of 84 genes involved in DNA-damage signaling by RT-PCR array. Fold differences of gene expressions with a cutoff of <0.5 (32D-RUNX1dC/32D-neo) are shown. (**d**) Relative mRNA expression levels of *Gadd45a* in Mock-, RUNX1dC-, D171N- and RUNX1b-transduced murine LSK cells (normalized to *Gapdh*). Data are means ± s.e.m. of triplicate experiments.

significantly lower (42%) in 32D-RUNX1dC cells than in 32D-neo cells (Supplementary Figure 2b). To examine if this result was relevant to normal LSK cells, we also examined the expression of *Gadd45a* in RUNX1dC-transduced LSK cells. RUNX1dC-transduced LSK cells showed significantly lower expression (44%) of *Gadd45a* than Mock-transduced LSK cells (Figure 3d). LSK cells, which were transduced with a RUNX1 mutant harboring a point mutation in the Runt homology domain (D171N)[19,21] also showed significantly lower (53%) expression of *Gadd45a* compared with Mock-transduced LSK

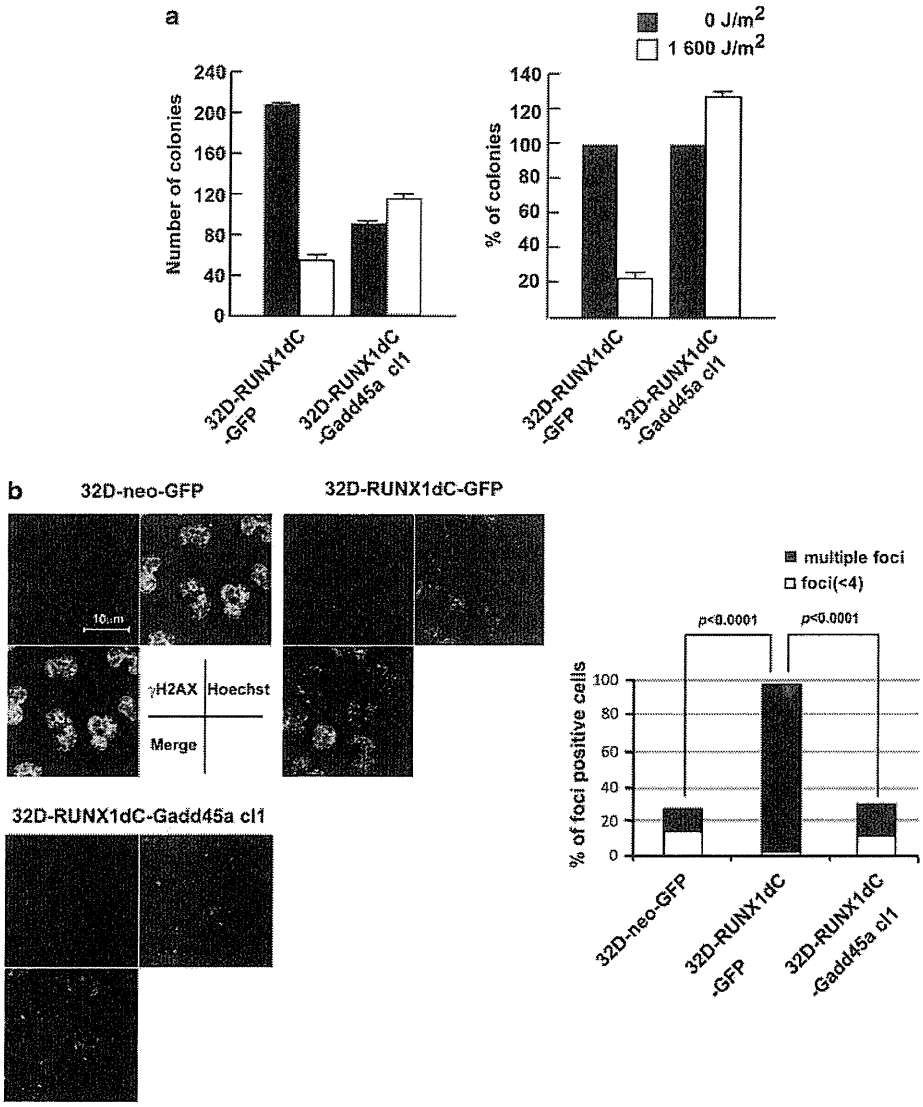

Figure 4 Exogenously expressed Gadd45a reduced γH2AX-positive foci in 32D-RUNX1dC. (**a**) Colony-forming ability of 32D-RUNX1dC-GFP and 32D-RUNX1dC-Gadd45a cl1 cells after UV-B treatment. Each bar shows absolute colony numbers (left panel) or the % colonies relative to those of non-treated cells (right panel). Data are means ± s.e.m. of triplicate experiments. (**b**) Accumulations of γH2AX foci in 32D-neo-GFP, 32D-RUNX1dC-GFP and 32D-RUNX1dC-Gadd45a cl1 cells 6 h after γ-ray treatment (left panel). The percentage of γH2AX foci-positive cells in 32D-neo-GFP, 32D-RUNX1dC-GFP and 32D-RUNX1dC-Gadd45a cl1 cells 6 h after γ-ray treatment are shown (right panel). Results are the average of three experiments. Open square indicates % of γH2AX foci-positive cells (with fewer than four foci per cell), and closed square indicates % of multiple foci-positive cells (four or more foci per cell).

cells (Figure 3d). Moreover, WT RUNX1-transduced LSK cells expressed more *Gadd45a*, an increase of 108% relative to Mock-transduced LSK cells (Figure 3d). To examine whether the impaired colony-forming ability of 32D-RUNX1dC cells attributed to the repressed expression of *Gadd45a* by RUNX1dC, we introduced the expression vector for Gadd45a into 32D-RUNX1dC cells, which was named 32D-RUNX1dC-Gadd45a (Supplementary Figure 3a). Consistent with the report from Perugini *et al.*,[27] Gadd45a overexpression reduced the cell proliferation ability at steady state (Figure 4a left panel). After UV-B treatment, exogenously expressed Gadd45a restored the colony-forming ability in 32D-RUNX1dC-Gadd45a cl1 cells (32D-RUNX1dC-GFP, 21.8%; 32D-RUNX1dC-Gadd45a cl1, 132%; Figure 4a right panel). Similar results were obtained from two other clones (Supplementary Figure 3b). Furthermore, we found exogenously expressed Gadd45a reduced γH2AX-positive foci in 32D-RUNX1dC-Gadd45a cl1 cells compared with 32D-RUNX1dC-GFP cells after UV-B treatment (Figure 4b). In addition, the reduction of γH2AX-positive foci in 32D-RUNX1dC-Gadd45a cl1 cells was also observed at steady state (Supplementary Figure 3c).

RUNX1 transcriptionally regulates Gadd45a expression

To analyze the mechanism by which RUNX1 regulates *Gadd45a* expression, we utilized luciferase assays using a human myeloid leukemia cell line UT-7/GM. Although there was no consensus sequence for RUNX binding in the 5′-flanking region of the human *GADD45A* gene, we found two RUNX-binding sequences neighboring the p53-binding site in

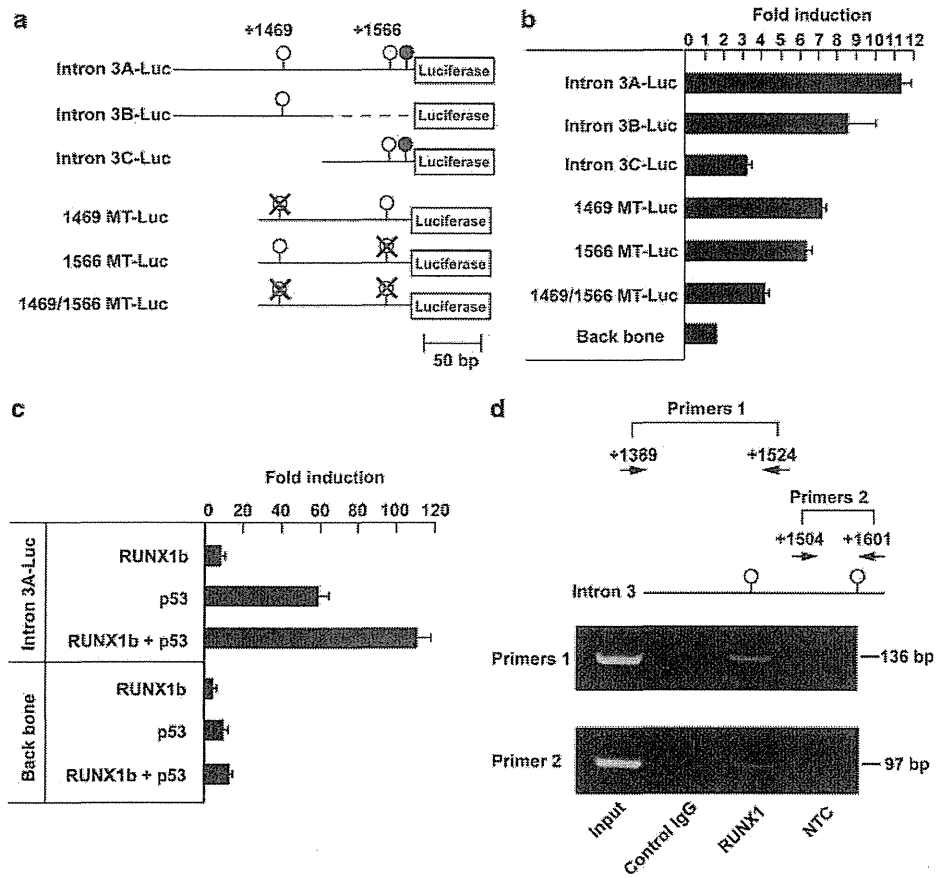

Figure 5 Analyses of transcriptional regulation of *GADD45A* by RUNX1. (**a**) Structures of human *GADD45A* luciferase reporter genes. Open circle indicates RUNX-binding sequences (at +1469 and +1566) and the closed circle indicates the reported p53-binding site in intron 3 of *GADD45A*. Crossed open circle indicates a mutation of the RUNX-binding sequence (TGTGGT changed into TGTTAG). (**b**) Reporter assays using human *GADD45A* luciferase reporter genes. Each bar indicates the fold induction of reporter activity induced by RUNX1b (relative to pRC-CMV control vector). UT-7/GM cells were transfected with 2 μg of each reporter gene (intron 3A-Luc (containing +1389–1601), intron 3B-Luc (+1389–1524), intron 3C-Luc (+1505–1601), 1469 MT-Luc, 1566 MT-Luc and 1469/1566 MT-Luc) or back bone plasmid, 0.5 μg of pRL-CMV-Rluc, 1 μg of CBFβ, and 2 μg of RUNX1b or pRC-CMV. Results shown are the means ± s.e.m. of triplicate experiments. (**c**) Co-expression experiment of RUNX1b and p53 using the intron 3A-Luc construct. Each bar indicates the fold induction of reporter activity induced by RUNX1b and/or p53 (relative to pRC-CMV control vector). Cells were transfected with 2 μg each of RUNX1b and/or p53 with 2 μg of intron 3A-Luc or Back bone plasmid, 0.5 μg of pRL-CMV-Rluc and 1 μg of CBFβ. Results shown are the means ± s.e.m. of triplicate experiments. (**d**) ChIP assays using the nuclear extract of UT-7/GM cells with the anti-RUNX1 Ab or control goat IgG. Two sets of closed arrows indicated primer positions in intron 3 of the *GADD45A* gene. Open circle indicates the RUNX-binding sequences and NTC means non-template control.

intron 3 of the *GADD45A* gene. Intron 3 is highly conserved between humans and rodents, and p53 transcriptionally activates *GADD45A* expression through this p53-binding site.[28,29] Therefore, we generated three types of luciferase reporter genes covering this region. Intron 3A-Luc contained the two RUNX-binding sequences (at +1469 and +1566) of the human *GADD45A* gene. Intron 3B-Luc contained only the upstream binding sequence (+1469) and intron 3C-Luc contained only the downstream binding sequence (+1566; Figure 5a). RUNX1b together with its heterodimerization partner CBFβ activated intron 3A-Luc, intron 3B-Luc and intron 3C-Luc 11.2-fold, 8.6-fold, and 3.2-fold, respectively (Figure 5b). The 1469 MT-Luc and 1566 MT-Luc constructs, which have one mutated RUNX-binding sequence (TGTGGT changed to TGTTAG), showed reduced reporter activity by RUNX1b compared with intron 3A-Luc (7.3-fold activation in 1469 MT-Luc and 6.1-fold activation in 1566 MT-Luc, Figures 5a and b). Furthermore, the 1469/1566 MT-Luc construct, which has two mutated RUNX-binding sequences, showed a 63% reduction of reporter activity by RUNX1 compared with intron 3A-Luc (4.1-fold activation). In addition, the co-expression experiment with RUNX1b and p53 revealed these two genes synergistically activate the intron 3A-Luc construct (only p53: 59.6-fold activation and p53 with RUNX1: 108.4-fold activation; Figure 5c). We also examined the change in intron 3A-Luc activation by RUNX1b and/or p53 after γ-ray irradiation; yet, there was no difference in reporter activities between γ-ray irradiated and non-irradiated UT-7/GM cells (data not shown). Next, we examined the co-expression effects of RUNX1 mutants on *GADD45A*-reporter activation with RUNX1b. We had to transfect high amount of DNA into test cells; therefore we utilized the adherent cell line, 293T, to perform the luciferase assay.[20] Single transduction experiment of RUNX1dC revealed RUNX1dC showed reduced *GADD45A*-reporter activity compared with the transduction of RUNX1b (10-fold activation in RUNX1b and 5-fold activation in RUNX1dC). In the case of the D171N mutant, the D171N mutant did not show the significant *GADD45A*-reporter activity (3.3-fold) compared with back-bone

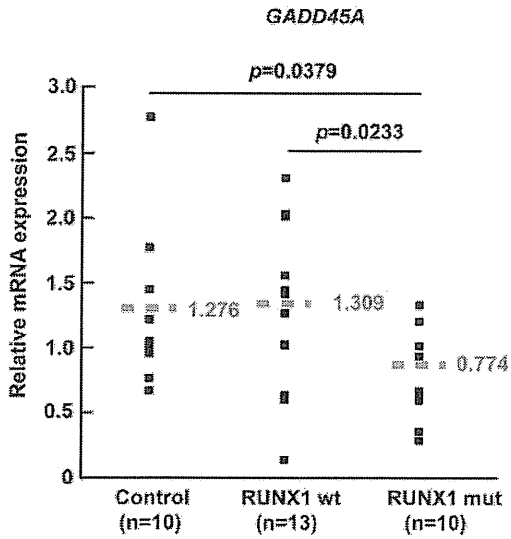

Figure 6 Expression levels of *GADD45A* in MDS/AML patients. Relative expression levels of *GADD45A* in BMMNCs from controls and MDS/AML patients with WT *RUNX1* (RUNX1 wt) or C-terminal mutations (RUNX1 mut) are shown. Horizontal bar and value denotes mean *GADD45A* expressions (normalized to *GAPDH*). The patients' characteristics are shown in Supplementary Table 2.

reporter activity (2.9-fold). In addition, we found RUNX1b-induced intron 3A-Luc activity was reduced to 55% by RUNX1dC and to 37% by the D171N mutant (Supplementary Figure 4). To test whether endogenous RUNX1 binds to the *GADD45A* gene *in vivo*, we conducted ChIP assays using the nuclear extract of UT-7/GM cells. As shown in Figure 5d, the two RUNX-binding sequences were immunoprecipitated with the anti-RUNX1 antibody but not by control IgG. Together, these data indicate that endogenous RUNX1 binds to two RUNX1-binding sites in intron 3 of the *GADD45A* gene, thereby regulating its transcription.

GADD45A expression is significantly decreased in MDS/AML patients harboring RUNX1-C-terminal mutations compared with those with WT RUNX1

Finally, we evaluated *GADD45A* expression in BM mononuclear cells from 23 MDS/AML patients with or without *RUNX1* C-terminal mutations and from 10 controls.[19] We found BM mononuclear cells from MDS/AML patients harboring *RUNX1*-C-terminal mutations had significantly lower *GADD45A* expression compared with those from MDS/AML patients with WT *RUNX1* ($P=0.0233$; Figure 6).

Discussion

We found RUNX1 transcriptionally regulates *Gadd45a*. In our experiment using LSK cells, the expression of *Gadd45a* was reduced to 44% of that of control cells by RUNX1dC (Figure 3d). This level of *Gadd45a* expression is roughly the same as that observed in *Gadd45a*$^{+/-}$ mice, which do not develop spontaneous tumors but are susceptible to tumor development in response to mutagens because of genomic instability.[30] Like *Gadd45a*$^{+/-}$ mice, heterozygous deletion of *RUNX1* predisposes mice to AML when accompanied by other gene alterations.[31] The similar phenotypes of *Gadd45a*$^{+/-}$ and *RUNX1*$^{+/-}$ mice raise the possibility that both molecules have closely related roles in maintaining genome stability. As for the relationship between RUNX1 and Gadd45a, Perugini *et al.*[27] recently reported that *GADD45A* expression was significantly downregulated in RUNX1-ETO-positive AML cells compared with normal controls. Although they demonstrated ERK1/2 signaling was involved in the repression of *GADD45A* in several AML cell lines, its mechanism was not analyzed in their study. In previous papers, RUNX1-ETO was shown to decrease the expression of several genes involved in the base excision repair pathway, such as oxoguanine DNA glycosylase and polymerase epsilon, thereby DNA damage accumulated.[32,33] Gadd45a functions in the nucleotide excision repair pathway through its interaction with proliferating cell nuclear antigen;[34–36] therefore, both base excision repair and nucleotide excision repair might be impaired in hematopoietic cells carrying RUNX1 mutations. Gadd45a also functions as a stress sensor, which is mediated by a complex interplay of physical interactions with other cellular proteins that are implicated in cell-cycle regulation and the response of cells to stress.[17] Gupta *et al.*[37] reported that Gadd45a-deficient hematopoietic cells demonstrated an impaired DDR response. They found myeloid-enriched BM cells from Gadd45a- or Gadd45b-deficient mice were defective in G2/M arrest following exposure to UV and VP-16 and these cells were sensitized to genotoxic-stress-induced apoptosis.[37] Similarly, we found that RUNX1dC-transduced LSK cells showed lower colony-forming ability than Mock-transduced LSK cells after UV-B exposure. Like RUNX1dC-transduced cells, *Gadd45a* expression was reduced in D171N-transduced LSK cells compared with Mock-transduced LSK cells (Figure 3d). The D171N mutant does not have DNA-binding ability, whereas it still maintains the ability to bind to CBFβ.[5] The co-expression experiment with D171N inhibited *GADD45A* reporter activation induced by RUNX1b (Supplementary Figure 4); therefore, it is possible that D171N inhibits the function of WT RUNX1 by trapping CBFβ. Differences in the DDR response between N-terminal in-frame type mutations (such as the D171N mutant) and C-terminal truncated mutations (such as the RUNX1dC) of *RUNX1* should be explored in a future study.

Gadd45a is a well known transcriptional target of p53.[29] p53 binds to the conserved sequence within intron 3 of the *GADD45A* gene in response to ionizing radiation.[29] Here, we showed that RUNX1 activates transcription of *GADD45A* through binding to two RUNX-binding sites neighboring the p53-binding site within intron 3 (Figure 5b). RUNX1 and p53 showed synergistic effects on intron3A-Luc activation (Figure 5c); therefore, these two molecules may cooperatively regulate *GADD45A* expression. In our experiment, however, γ-ray irradiation did not influence intron 3A-Luc activation by RUNX1 and/or p53. We are now trying to examine the cooperating effect of RUNX1 and p53 on DDR response, including *GADD45A* regulation, using a more physiological setting.

MDS patients with a *RUNX1* mutation frequently present with more advanced diseases and *RUNX1* mutations are considered to be markers of a poor prognosis.[19,38,39] We speculate that a RUNX1 mutation may be a cause of additional mutation(s) through the impaired DDR response. In future studies, whole genome analysis of MDS/AML samples harboring RUNX1 mutations would clarify the role of RUNX1 mutations in the occurrence of genetic abnormalities in these patients.

In conclusion, we demonstrated that a *RUNX1* C-terminal deletion mutant attenuates the DDR response to environmental and physiological stresses in LSK cells. As a possible explanation

for this mechanism, we found a novel role for RUNX1 in the transcriptional regulation of *Gadd45a*. The impaired Gadd45a function leads to genomic instability; therefore, Gadd45a dysfunction induced by *RUNX1* mutations can cause the additional mutation(s) required for multi-step leukemogenesis. Further studies on RUNX1/Gadd45a would be useful to understand the pathophysiology of MDS/AML patients harboring RUNX1 abnormalities and to prevent disease progression.

Conflict of interest

The authors declare no conflict of interest.

Acknowledgements

We thank the Department of Dermatology, Osaka University Graduate School of Medicine for help with UV-B-exposure experiments, Y Sowa and T Sakai for help with reporter assays of *Gadd45a*, and J Yamauchi for technical advice. We appreciate discussions with and suggestions of C Masutani, K Oritani, T Yokota and S Ezoe. This research was supported in part by a Grant-in Aid for Scientific Research (C) (to Y Satoh), a Grant-in Aid for Scientific Research (B) (to I Matsumura) from MEXT and by the Sankyo Foundation of Life Science.

References

1 Hirai H. Molecular mechanisms of myelodysplastic syndrome. *Jpn J Clin Oncol* 2003; **33**: 153–160.
2 Quesnel B, Guillerm G, Vereecque R, Wattel E, Preudhomme C, Bauters F *et al.* Methylation of the p15(INK4b) gene in myelodysplastic syndromes is frequent and acquired during disease progression. *Blood* 1998; **91**: 2985–2990.
3 Sugimoto K, Hirano N, Toyoshima H, Chiba S, Mano H, Takaku F *et al.* Mutations of the p53 gene in myelodysplastic syndrome (MDS) and MDS-derived leukemia. *Blood* 1993; **81**: 3022–3026.
4 Russell M, List A, Greenberg P, Woodward S, Glinsmann B, Parganas E *et al.* Expression of EVI1 in myelodysplastic syndromes and other hematologic malignancies without 3q26 translocations. *Blood* 1994; **84**: 1243–1248.
5 Harada Y, Harada H. Molecular pathways mediating MDS/AML with focus on AML1/RUNX1 point mutations. *J Cell Physiol* 2009; **220**: 16–20.
6 Yoneda-Kato N, Look AT, Kirstein MN, Valentine MB, Raimondi SC, Cohen KJ *et al.* The t(3;5)(q25.1;q34) of myelodysplastic syndrome and acute myeloid leukemia produces a novel fusion gene, NPM-MLF1. *Oncogene* 1996; **12**: 265–275.
7 Delhommeau F, Dupont S, Della Valle V, James C, Trannoy S, Masse A *et al.* Mutation in TET2 in myeloid cancers. *N Engl J Med* 2009; **360**: 2289–2301.
8 Speck NA, Gilliland DG. Core-binding factors in haematopoiesis and leukaemia. *Nat Rev Cancer* 2002; **2**: 502–513.
9 Tang JL, Hou HA, Chen CY, Liu CY, Chou WC, Tseng MH *et al.* AML1/RUNX1 mutations in 470 adult patients with *de novo* acute myeloid leukemia: prognostic implication and interaction with other gene alterations. *Blood* 2009; **114**: 5352–5361.
10 Song WJ, Sullivan MG, Legare RD, Hutchings S, Tan X, Kufrin D *et al.* Haploinsufficiency of CBFA2 causes familial thrombocytopenia with propensity to develop acute myelogenous leukaemia. *Nat Genet* 1999; **23**: 166–175.
11 Ichikawa M, Asai T, Saito T, Seo S, Yamazaki I, Yamagata T *et al.* AML-1 is required for megakaryocytic maturation and lymphocytic differentiation, but not for maintenance of hematopoietic stem cells in adult hematopoiesis. *Nat Med* 2004; **10**: 299–304.
12 Higuchi M, O'Brien D, Kumaravelu P, Lenny N, Yeoh EJ, Downing JR. Expression of a conditional AML1-ETO oncogene bypasses embryonic lethality and establishes a murine model of human t(8;21) acute myeloid leukemia. *Cancer Cell* 2002; **1**: 63–74.
13 Jackson SP, Bartek J. The DNA-damage response in human biology and disease. *Nature* 2009; **461**: 1071–1078.
14 Lindahl T, Barnes DE. Repair of endogenous DNA damage. *Cold Spring Harb Symp Quant Biol* 2000; **65**: 127–133.
15 Hoeijmakers JH. Genome maintenance mechanisms for preventing cancer. *Nature* 2001; **411**: 366–374.
16 Kundu M, Compton S, Garrett-Beal L, Stacy T, Starost MF, Eckhaus M *et al.* Runx1 deficiency predisposes mice to T-lymphoblastic lymphoma. *Blood* 2005; **106**: 3621–3624.
17 Liebermann DA, Hoffman B. Gadd45 in stress signaling. *J Mol Signal* 2008; **3**: 15.
18 Bennett JM, Catovsky D, Daniel MT, Flandrin G, Galton DA, Gralnick HR *et al.* Proposals for the classification of the myelodysplastic syndromes. *Br J Haematol* 1982; **51**: 189–199.
19 Harada H, Harada Y, Niimi H, Kyo T, Kimura A, Inaba T. High incidence of somatic mutations in the AML1/RUNX1 gene in myelodysplastic syndrome and low blast percentage myeloid leukemia with myelodysplasia. *Blood* 2004; **103**: 2316–2324.
20 Satoh Y, Matsumura I, Tanaka H, Ezoe S, Fukushima K, Tokunaga M *et al.* AML1/RUNX1 works as a negative regulator of c-Mpl in hematopoietic stem cells. *J Biol Chem* 2008; **283**: 30045–30056.
21 Harada H, Harada Y, Tanaka H, Kimura A, Inaba T. Implications of somatic mutations in the AML1 gene in radiation-associated and therapy-related myelodysplastic syndrome/acute myeloid leukemia. *Blood* 2003; **101**: 673–680.
22 Tanaka T, Tanaka K, Ogawa S, Kurokawa M, Mitani K, Nishida J *et al.* An acute myeloid leukemia gene, AML1, regulates hemopoietic myeloid cell differentiation and transcriptional activation antagonistically by two alternative spliced forms. *EMBO J* 1995; **14**: 341–350.
23 Rogakou EP, Pilch DR, Orr AH, Ivanova VS, Bonner WM. DNA double-stranded breaks induce histone H2AX phosphorylation on serine 139. *J Biol Chem* 1998; **273**: 5858–5868.
24 Mah LJ, El-Osta A, Karagiannis TC. gammaH2AX: a sensitive molecular marker of DNA damage and repair. *Leukemia* 2010; **24**: 679–686.
25 Nojima K, Hochegger H, Saberi A, Fukushima T, Kikuchi K, Yoshimura M *et al.* Multiple repair pathways mediate tolerance to chemotherapeutic cross-linking agents in vertebrate cells. *Cancer Res* 2005; **65**: 11704–11711.
26 Mori T, Nakane M, Hattori T, Matsunaga T, Ihara M, Nikaido O. Simultaneous establishment of monoclonal antibodies specific for either cyclobutane pyrimidine dimer or (6-4)photoproduct from the same mouse immunized with ultraviolet-irradiated DNA. *Photochem Photobiol* 1991; **54**: 225–232.
27 Perugini M, Kok CH, Brown AL, Wilkinson CR, Salerno DG, Young SM *et al.* Repression of Gadd45alpha by activated FLT3 and GM-CSF receptor mutants contributes to growth, survival and blocked differentiation. *Leukemia* 2009; **23**: 729–738.
28 Hollander MC, Alamo I, Jackman J, Wang MG, McBride OW, Fornace Jr AJ. Analysis of the mammalian gadd45 gene and its response to DNA damage. *J Biol Chem* 1993; **268**: 24385–24393.
29 Kastan MB, Zhan Q, el-Deiry WS, Carrier F, Jacks T, Walsh WV *et al.* A mammalian cell cycle checkpoint pathway utilizing p53 and GADD45 is defective in ataxia-telangiectasia. *Cell* 1992; **71**: 587–597.
30 Hollander MC, Sheikh MS, Bulavin DV, Lundgren K, Augeri-Henmueller L, Shehee R *et al.* Genomic instability in Gadd45a-deficient mice. *Nat Genet* 1999; **23**: 176–184.
31 Yamashita N, Osato M, Huang L, Yanagida M, Kogan SC, Iwasaki M *et al.* Haploinsufficiency of Runx1/AML1 promotes myeloid features and leukaemogenesis in BXH2 mice. *Br J Haematol* 2005; **131**: 495–507.
32 Krejci O, Wunderlich M, Geiger H, Chou FS, Schleimer D, Jansen M *et al.* p53 signaling in response to increased DNA damage sensitizes AML1-ETO cells to stress-induced death. *Blood* 2008; **111**: 2190–2199.
33 Alcalay M, Meani N, Gelmetti V, Fantozzi A, Fagioli M, Orleth A *et al.* Acute myeloid leukemia fusion proteins deregulate genes involved in stem cell maintenance and DNA repair. *J Clin Invest* 2003; **112**: 1751–1761.
34 Vairapandi M, Balliet AG, Hoffman B, Liebermann DA. GADD45b and GADD45g are cdc2/cyclinB1 kinase inhibitors with a role in S

and G2/M cell cycle checkpoints induced by genotoxic stress. *J Cell Physiol* 2002; **192**: 327–338.
35 Smith ML, Chen IT, Zhan Q, Bae I, Chen CY, Gilmer TM *et al.* Interaction of the p53-regulated protein Gadd45 with proliferating cell nuclear antigen. *Science* 1994; **266**: 1376–1380.
36 Smith ML, Ford JM, Hollander MC, Bortnick RA, Amundson SA, Seo YR *et al.* p53-mediated DNA repair responses to UV radiation: studies of mouse cells lacking p53, p21, and/or gadd45 genes. *Mol Cell Biol* 2000; **20**: 3705–3714.
37 Gupta M, Gupta SK, Balliet AG, Hollander MC, Fornace AJ, Hoffman B *et al.* Hematopoietic cells from Gadd45a- and Gadd45b-deficient mice are sensitized to genotoxic-stress-induced apoptosis. *Oncogene* 2005; **24**: 7170–7179.
38 Steensma DP, Gibbons RJ, Mesa RA, Tefferi A, Higgs DR. Somatic point mutations in RUNX1/CBFA2/AML1 are common in high-risk myelodysplastic syndrome, but not in myelofibrosis with myeloid metaplasia. *Eur J Haematol* 2005; **74**: 47–53.
39 Chen CY, Lin LI, Tang JL, Ko BS, Tsay W, Chou WC *et al.* RUNX1 gene mutation in primary myelodysplastic syndrome—the mutation can be detected early at diagnosis or acquired during disease progression and is associated with poor outcome. *Br J Haematol* 2007; **139**: 405–414.

Supplementary Information accompanies the paper on the Leukemia website (http://www.nature.com/leu)

bjh research paper

Chromosome abnormalities in advanced stage T-cell lymphoblastic lymphoma of children and adolescents: a report from Japanese Paediatric Leukaemia/Lymphoma Study Group (JPLSG) and review of the literature

Masahiro Sekimizu,[1] Shosuke Sunami,[2] Atsuko Nakazawa,[3] Yasuhide Hayashi,[4] Yuri Okimoto,[5] Akiko M. Saito,[6] Keizo Horibe,[1,7] Masahito Tsurusawa[8] and Tetsuya Mori[9]

[1]Department of Paediatrics, National Hospital Organization Nagoya Medical Centre, Aichi, [2]Department of Paediatrics, Narita Red Cross Hospital, Chiba, [3]Department of Pathology, National Centre for Child Health and Development, Tokyo, [4]Department of Haematology/Oncology, Gunma Children's Medical Centre, Gunma, [5]Division of Haematology and Oncology, Chiba Children's Hospital, Chiba, [6]Department of Clinical Research Promotion, Clinical Research Centre, National Hospital Organization Nagoya Medical Centre, [7]Clinical Research Centre, National Hospital Organization Nagoya Medical Centre, [8]Department of Paediatrics, Aichi Medical University, Aichi, and [9]Division of Paediatric Oncology, National Centre for Child Health and Development, Tokyo, Japan

Received 4 April 2011; accepted for publication 24 May 2011

Correspondence: Masahiro Sekimizu, Department of Paediatrics, National Hospital Organization Nagoya Medical Centre, 4-1-1 Sannomaru, Naka-ku, Nagoya, Aichi 460-0001, Japan. E-mail: sekimizu@nnh.hosp.go.jp

Summary

T-cell acute lymphoblastic leukaemia (T-ALL) and T-cell lymphoblastic lymphoma (T-LBL) are combined into one category as T lymphoblastic leukaemia/lymphoma in the current World Health Organization (WHO) classification. However, there is still ongoing discussion on whether T-ALL and T-LBL are two separate entities or represent two variant phenotypes of the same disease. Cytogenetic analysis has been used to identify the molecular background of haematological malignancies. To compare the distribution of chromosomal abnormalities of T-ALL and T-LBL, large series of cytogenetic data are required, but are absent in T-LBL in contrast to the abundant data in T-ALL. Among 111 T-LBL cases in our clinical trial, we obtained complete cytogenetic data from 56 patients. The comparison between our cytogenetic findings and those from three published T-LBL studies revealed no significant difference. However, meta-analysis showed that translocations involving chromosome region 9q34 were significantly more common in T-LBL than in T-ALL. In particular, four out of the 92 T-LBL cases, but none of the 523 paediatric T-ALL cases, showed translocation t(9;17)(q34;q22–23) ($P = 0{\cdot}0004$). Further studies are needed for the possible linkage between abnormal expression of genes located at 9q34 and/or 17q22–23 and the unique 'lymphoma phenotype' of T-LBL.

Keywords: T-cell lymphoma, child, non-Hodgkin lymphoma, cancer cytogenetics, leukaemia.

In children and adolescents, precursor T lymphoblastic neoplasms have been classified into two diseases: T-cell acute lymphoblastic leukaemia (T-ALL) and T-cell lymphoblastic lymphoma (T-LBL). Although the current World Health Organization (WHO) classification designates both malignancies as T lymphoblastic leukaemia/lymphoma (Borowitz & Chan, 2008), there is continuing discussion on whether T-ALL and T-LBL are two separate entities or whether they represent two different clinical presentations of the same disease. They show overlapping clinical, pathological and immunophenotypic features. In general, the word 'lymphoma' is used if there is a bulky mass in the mediastinum or elsewhere, with less peripheral blood and bone marrow (BM) involvement. Most study groups distinguish between leukaemia and lymphoma on the basis of the extent of BM involvement: patients with <25% lymphoblasts in the BM are diagnosed with lymphoblastic lymphoma; in cases

First published online 21 June 2011
doi:10.1111/j.1365-2141.2011.08788.x

of 25% or more BM blasts, the diagnosis is leukaemia. While this distinction may appear somewhat arbitrary, a notable observation is that T-LBL patients with large mediastinal masses frequently exhibit little, if any, evidence of tumour dissemination and BM involvement, but the molecular background for this difference is unknown.

Chromosomal analysis has been widely used as a primary step that is required to narrow down the responsible genes that define a disease entity. For instance, discovery of Ph chromosome led to the identification of the chimeric *BCR/ABL1* gene, which is responsible for and defines chronic myeloid leukaemia. Compared with T-ALL, chromosomal abnormalities in T-LBL are not well defined. Reports in the literature and current textbooks claim that the typical chromosomal aberrations reported in T-ALL can also be found in T-LBL (Borowitz & Chan, 2008). However, there are no large series of cytogenetic data on T-LBL (Burkhardt, 2010).

This study aimed to fill the gap regarding cytogenetic data in T-LBL and compare the cytogenetic findings of T-ALL and T-LBL, which may lead to identification of the molecular background behind phenotypical differences between the two disease entities.

Study patients

From November 2004 to October 2010, 154 eligible children (aged 1–18 years) with newly diagnosed advanced stage LBL (Murphy stages III and IV) (Murphy, 1980) were entered in the Japanese Paediatric Leukaemia/Lymphoma Study Group (JPLSG) ALB-NHL03 study (UMIN000002212, http://www.umin.ac.jp/ctr/index-j.htm). Patients with primary immunodeficiencies, Down syndrome and T-cell diseases as second malignancies were excluded. The ethics committee of each participating institute approved the study protocol.

Cytogenetic analysis

Cytogenetic analysis was performed on cell suspensions obtained from 31 tumour/lymph nodes, 19 pleural effusions and six bone marrow samples. The methods of chromosome preparation for cytogenetic analysis are described elsewhere (Sanger *et al*, 1987; Horsman *et al*, 2001). Karyotypes are described according to the International System for Human Cytogenetic Nomenclature (ISCN) (Shaffer & Tommerup, 2005). Only those cases with abnormal cytogenetic study results, defined as two or more cells with the same structural abnormality or the same numerical gain, three or more cells with the same numerical loss or isolated cells with disease-associated abnormalities, were eligible for inclusion in this study.

Statistical methods

Two-tailed Fisher's exact test was used to analyse the patients' characteristics and the frequency of each chromosome abnormality. Significant differences in the analysis of he frequency of each chromosome abnormality were determined by the two-tailed Fisher's exact test with Bonferroni correction comparison. The P value threshold for inclusion of a new variable was chosen to be $P < 0{\cdot}003$ in this analysis (0·05/17, after Bonferroni correction). A review of T-LBL and T-ALL karyotypes reported in the literature was obtained from a PubMed search and information on chromosome abnormalities and gene fusions was obtained from Mitelman Database of Chromosome Aberrations and Gene Fusions in Cancer (http://cgap.nci.nih.gov/Chromosomes/Mitelman).

Results

Patient characteristics

A total of 154 children were enrolled on JPLSG ALB-NHL03 protocols; 111 cases were T-LBL. Among 111 T-LBL cases, the study population for the current analysis included 56 patients for whom complete cytogenetic data were obtained. With respect to presenting features, patients with reviewed and accepted cytogenetic data were similar to both those without accepted cytogenetic data and the entire cohort of concurrently enrolled T-lineage LBL patients (Table S1).

Frequency of chromosomal abnormalities

Multiple chromosome abnormalities were identified in 31 patients (45%). Structural chromosome abnormalities were identified in 29 patients (52%), and numerical chromosome abnormalities were identified in 18 patients (32%). Ploidy results included pseudodiploid in 14 patients (25%), hypodiploid in three patients (5%), hyperdiploid with 47–50 chromosomes in 10 patients (18%), hyperdiploid with more than 50 chromosomes in four patients (7%) and diploid in 25 patients (45%) (Table S2).

All of the hypodiploid cases had 43–45 chromosomes; none had a near-haploid karyotype. Of the four cases with more than 50 chromosomes, two had near-tetraploid karyotypes. The frequencies of ploidy groups in this series are compared with those reported in other series of karyotyped T-LBL patients and paediatric T-ALL (Table S2). Structural chromosome abnormalities were identified in 29 patients (52%). In the current study, seven patients (13% of those with abnormal karyotypes) exhibited a rearrangement at one or more of the chromosome bands (7p15, 7q32–36 and/or 14q11–13) that are the locations of T-cell receptor chain genes. Rearrangements in the 14q11–13 region, in which the T-cell receptor α/δ chain genes are located, were present in three patients (5%) of the karyotypically abnormal cases in this series (Table S2). Structural abnormalities involving chromosome region 9q34 were identified in nine patients (16%). Translocations involving chromosome region 9q34 were identified in three patients (5%) (t(9;17)(q34;q22), t(7;9)(q34;q34) and t(2;9)(q23;q34)). In comparison between cytogenetic findings in the current data and combined data of three published reports (Burkhardt

et al, 2006; Lones *et al*, 2007; Uyttebroeck *et al*, 2007; Table S1), the frequencies of numerical and structural cytogenetic abnormalities in T-LBL and T-ALL had no significant difference (Table S2).

We compared the cytogenetic findings in the current study with the published reports from the three largest-scale studies on T-LBL (Burkhardt *et al*, 2006; Lones *et al*, 2007; Uyttebroeck *et al*, 2007; Table S3) and those from the two largest-scale studies on T-ALL combined (Heerema *et al*, 1998; Schneider *et al*, 2000; Table S3) (Table I). The frequencies of almost all of the cytogenetic abnormalities in T-LBL and T-ALL had no significant difference, but translocation involving chromosome region 9q34 was significantly more common in T-LBL than in T-ALL ($P = 0{\cdot}0004$, Table S3) and translocation t(9;17) was also more common in T-LBL (4%, 4/92) than in T-ALL (0%, 0/523, $P = 0{\cdot}0004$) (Table I).

The current study included a patient with translocation t(9;17)(q34;q22). As far as we could tell from the consulted published reports, all T-LBL patients with translocation t(9;17) presented with a mediastinal mass and without any bone marrow involvement (Kaneko *et al*, 1988; Shikano *et al*, 1992) (Table II).

Table I. Comparison of cytogenetic findings between T-LBL and T-ALL.

	T-LBL		T-ALL		
	n	%	*n*	%	*P* value
Total	92		523		
Normal karyotype†	36	39	219	42	0·6478
Abnormal karyotype	56	61	304	58	0·6478
Hypodiploid	4	4	20	4	0·9999
Pseudodiploid	30	33	204	39	0·2000
Hyperdiploid(47–50)	18	20	64	12	0·0328
Hyperdiploid(>50)	4	4	16	3	0·5217
Any translocation	26	28	177	34	0·3367
Any del chrome.	19	21	160	31	0·0328
Any der chrome.	4	4	58	11	0·0583
del(6q)	6	7	69	13	0·0833
Loss of 9p	10	11	44	8	0·5487
Any 14q11–13 abnormality	10	11	72	14	0·5100
Any 7q32–36 abnormality	7	8	35	7	0·8220
Any translocation including 9q34	8	9	7	1	0·0004*
t(7;10)	1	1	2	0	0·3855
t(10;11)	1	1	8	2	0·9999
t(9;17)	4	4	0	0	0·0004*

†Includes one Klinefelter syndrome, and one inv(9) without other abnormality in current report.

The *P* value threshold for inclusion of a new variable was chosen to be 0·003 (0·05/17, after Bonferroni correction). *$P < 0{\cdot}003$.

T-LBL: current study (JPLSG ALB-NHL03) combined with three published reports(Burkhardt *et al*, 2006; Lones *et al*, 2007; Uyttebroeck *et al*, 2007).

T-ALL: combined two published reports (Heerema *et al*, 1998; Schneider *et al*, 2000).

Discussion

This is the largest study involving cytogenetic analysis of T-LBL and the first study to directly compare cytogenetic findings of T-LBL and T-ALL. The frequencies of almost all of the cytogenetic abnormalities in both entities were found to have no significant difference, but translocation involving chromosome region 9q34 was significantly more common in T-LBL than in T-ALL. The current study included a patient with unique translocation t(9;17)(q34;q22). Interestingly, four out of the 92 T-LBL cases, but none of the 523 paediatric T-ALL cases, showed this translocation ($P = 0{\cdot}0004$) (Table I). Translocation t(9;17) has been reported in several haematological diseases, such as precursor B-cell ALL (Coyaud *et al*, 2010), acute myeloid leukaemia (Mrózek *et al*, 2001), chronic myeloid leukaemia (DeAngelo *et al*, 2004), chronic lymphocytic leukaemia (Michaux *et al*, 2005), diffuse large B-cell lymphoma (Hammond *et al*, 1992) and follicular lymphoma (Aamot *et al*, 2007), but these breakpoints, 9q34 and 17q22–23, are limited in the cases of T-LBL (http://cgap.nci.nih.gov/Chromosomes/Mitelman). These results imply a linkage between abnormal expression of genes located at 9q34 and/or 17q22–23 and the unique phenotypes of the T-LBL mentioned above.

Cytogenetic analysis has been used to identify the molecular background of haematological malignancies. To compare the distribution of chromosomal abnormalities of T-ALL and T-LBL, large series of cytogenetic data are required, but are absent in T-LBL in contrast to the abundant data in T-ALL. Three recent series of cytogenetic data on paediatric T-LBL have been published, reporting the cytogenetic findings in 13, 11 and 12 paediatric T-LBL cases (Burkhardt *et al*, 2006; Lones *et al*, 2007; Uyttebroeck *et al*, 2007). Thus, this study can play a role to fill the gap of cytogenetic data on T-LBL.

Translocation involving chromosome region 9q34 was found to be significantly more common in T-LBL than in T-ALL (Table I). Among genes located in the 9q34 region, *SET*, *PKN3*, *ABL1*, *NUP214* and *NOTCH1* have previously been implicated in malignancy, with *SET*, *ABL1*, *NUP214* and *NOTCH1* being implicated in leukemogenesis (Ellisen *et al*, 1991; van Vlierberghe *et al*, 2008; Hagemeijer & Graux, 2010).

An oncogenic *SET-NUP214* fusion gene has been reported in a case of acute undifferentiated leukaemia with a reciprocal translocation t(9;9)(q34; q34) (von Lindern *et al*, 1992) and NK adult acute myeloid leukaemia as a result of a cryptic deletion of 9q34 (Rosati *et al*, 2007). van Vlierberghe *et al* (2008) identified the *SET-NUP214* fusion gene in three patient samples out of 92 paediatric cases of T-cell leukaemia. *SET-NUP214* may contribute to T-ALL pathogenesis by inhibition of T-cell maturation through the transcriptional activation of the *HOXA* genes (van Vlierberghe *et al*, 2008). However, the frequency of this mutation in T-LBL is unknown.

NOTCH1, previously termed *TAN1*, was discovered as a partner gene in T-ALL with a translocation t(7;9)(q34;q34.3), and was found in <1% of T-ALLs (Ellisen *et al*, 1991). Several

Table II. Clinical characteristics and detailed karyotype data in T-LBL patients with t(9;17).

	Age (years)	Sex	Tumour site	Stage	BM blast %	Karyotype
Kaneko *et al* (1988)	14	F	Mediastinum	III	0	46,XX,t(9;17)(q34;q23)
	15	M	Mediastinum	III	0	46,XY,-9,del(6)(q13q21),t(9;17)(q34;q23),+der(9)t(9;17)(q34;q23)
	10	M	Mediastinum	III	0	47,XY,+19,t(9;17)(q34;q23)
Shikano *et al* (1992)	14	F	Mediastinum	III	0	46,XX,t(9;17)(q34;q23)
	7	M	Mediastinum	III	0	49,XY-l,+der(l)t(l;?)(p36;?),t(9;17)(q34;q23),+14,+marl,+mar2
	5	F	Mediastinum	III	0	47,XX,t(9;17)(q34;q23),+der(17)t(9;17)(q34;q23)
Burkhardt *et al* (2006)	ND	ND	ND	ND	ND	46,XX,del(6)(q1?2q1?6),t(9;17)(q34;q22)
	ND	ND	ND	ND	ND	47,XX,t(9;17)(q34;q22),+20
Lones *et al* (2007)	8	M	Mediastinum	III	0	47,XY,t(9;17)(q3?4;q2?3),+20
Current study	7	M	Mediastinum	III	0	46,XY,t(9;17)(q34;q22)

ND, no data available.

study groups reported *NOTCH1* mutations in 31–62% of T-ALL patients (Weng *et al*, 2004; Breit *et al*, 2006; van Grotel *et al*, 2006; Zhu *et al*, 2006; Malyukova *et al*, 2007; Asnafi *et al*, 2009; Gedman *et al*, 2009; Park *et al*, 2009). In contrast, only two studies reported *NOTCH1* mutation analyses in T-LBL: Park *et al* (2009) reported *NOTCH1* mutations in six out of 14 paediatric T-LBL patients (43%), and Baleydier *et al* (2008) reported mutations in six out of nine paediatric T-LBL (66%), with 32 adult patients with *NOTCH1* mutations in 16 cases (54% in all patients) (Baleydier *et al*, 2008). According to these reports, the frequencies of *NOTCH1* mutation were not significantly different between T-LBL and T-ALL.

ABL1 fusion genes have been identified that provide proliferation and survival advantage to lymphoblasts. *NUP214-ABL1*, *EML1-ABL1*, *BCR-ABL1* and *ETV6-ABL1* chimeric genes have been reported. The most frequent one in T-ALL is the *NUP214-ABL*1 fusion gene, which has been identified in 6% of cases, in both children and adults (Graux *et al*, 2009). In addition, using an oligonucleotide microarray, *ABL1* overexpression was identified in 8% of cases in T-ALL (Chiaretti *et al*, 2007). Our review of these published reports indicated that the frequency of ABL1 mutation in T-LBL is unknown.

Raetz *et al* (2006) analysed the gene expression profiles of ten T-ALL BM samples and nine T-LBL samples using a microarray. They identified 133 genes for which the expression levels differed between T-LBL and T-ALL. *ZNF79* (encoding zinc finger protein 79) and *ABL1*, both located in chromosome region 9q34, were included in these genes and showed at least twofold higher overexpression in T-LBL than that in T-ALL. Additionally, *MED13* (previously termed *THRAP1*), which is located in 17q22-q23, also showed at least twofold higher overexpression in T-LBL than that in T-ALL (Raetz *et al*, 2006). Taking these findings together, it is possible that *ZNF79*, *ABL1* or *THRAP1* as well as other genes at 9q34 and 17q22–23 are involved in the 'lymphoma phenotype' such as a bulky mass in the mediastinum and minimal BM involvement. These findings need further study to determine if this linkage constitutes a unique 'lymphoma phenotype'.

Acknowledgements

The authors are thankful to the participating paediatric oncologists in this study for providing the clinical data. This work was supported by a grant for Cancer Research and a grant for Research on Children and Families from the Ministry of Health, Labour and Welfare of Japan. We thank Drs Toshiki I. Saito (Nagoya Medical Centre, Aichi), and Yuichi Taneyama (Chiba Children's Hospital, Chiba) for supporting this study.

Authorship

MS designed the study, prepared the data file, performed the analysis, interpreted data and wrote the manuscript. SS is a lead principal investigator for the JPLSG ALB-NHL03 study. AN contributed to pathological diagnosis. YH contributed to chromosome analysis. YO is a principal investigator contributing a patient to this study. AMS contributed to statistical analysis. KH received a research grant from the Ministry of Health, Labour and Welfare of Japan. MT is a chairperson of JPLSG. TM is a chairperson of JPLSG lymphoma committee. SS, KH, MT and TM were primarily responsible for the study design, data analysis and interpretation of the data. All authors approved the final manuscript.

Disclosure

The authors declare no competing financial interests.

Supporting Information

Additional Supporting Information may be found in the online version of this article:

Table S1. Respective clinical characteristics with and without karyotype data in 111 T-LBL patients in the current study.

Table S2. Comparison of cytogenetic findings in T-LBL between current study and combined data of three published reports.

Table S3. Published data of cytogenetic findings in T-LBL and T-ALL.

References

Aamot, H.V., Torlakovic, E.E., Eide, M.B., Holte, H. & Heim, S. (2007) Non-Hodgkin lymphoma with t(14;18): clonal evolution patterns and cytogenetic-pathologic-clinical correlations. *Journal of Cancer Research and Clinical Oncology*, 133, 455–470.

Asnafi, V., Buzyn, A., Le Noir, S., Baleydier, F., Simon, A., Beldjord, K., Reman, O., Witz, F., Fagot, T., Tavernier, E., Turlure, P., Leguay, T., Huguet, F., Vernant, J.P., Daniel, F., Bene, M.C., Ifrah, N., Thomas, X., Dombret, H. & Macintyre, E. (2009) NOTCH1/FBXW7 mutation identifies a large subgroup with favorable outcome in adult T-cell acute lymphoblastic leukemia (T-ALL): a Group for Research on Adult Acute Lymphoblastic leukemia (GRAALL) study. *Blood*, 113, 3918–3924.

Baleydier, F., Decouvelaere, A.V., Bergeron, J., Gaulard, P., Canioni, D., Bertrand, Y., Lepretre, S., Petit, B., Dombret, H., Beldjord, K., Molina, T., Asnafi, V. & Macintyre, E. (2008) T cell receptor genotyping and HOXA/TLX1 expression define three T lymphoblastic lymphoma subsets which might affect clinical outcome. *Clinical Cancer Research*, 14, 692–700.

Borowitz, M. & Chan, J. (2008) WHO Classification of Tumours of Haematopoietic and Lymphoid Tissues. In: T lymphoblatic leukaemia/lymphoma (ed. by S. Swerdlow, E. Campo, N. Harris, E. Jaffe, S. Pileri, H. Stein, J. Thiele & J. Vardiman), pp. 176–178. Internationa Agency for Resarchon Cancer, Lyon.

Breit, S., Stanulla, M., Flohr, T., Schrappe, M., Ludwig, W.D., Tolle, G., Happich, M., Muckenthaler, M.U. & Kulozik, A.E. (2006) Activating NOTCH1 mutations predict favorable early treatment response and long term outcome in child-hood precursor T-cell lymphoblastic leukemia. *Blood*, 108, 1151–1157.

Burkhardt, B. (2010) Paediatric lymphoblastic T-cell leukaemia and lymphoma: one or two diseases? *British Journal of Haematology*, 149, 653–668.

Burkhardt, B., Bruch, J., Zimmermann, M., Strauch, K., Parwaresch, R., Ludwig, W.D., Harder, L., Schlegelberger, B., Mueller, F., Harbott, J. & Reiter, A. (2006) Loss of heterozygosity on chromosome 6q14–q24 is associated with poor outcome in children and adolescents with T-cell lymphoblastic lymphoma. *Leukemia*, 20, 1422–1429.

Chiaretti, S., Tavolaro, S., Ghia, E.M., Ariola, C., Matteucci, C., Elia, L., Maggio, R., Messina, M., Ricciardi, M.R., Vitale, A., Ritz, J., Mecucci, C., Guarini, A. & Foa, R. (2007) Characterization of ABL1 expression in adult T-cell acute lymphoblastic leukemia by oligonucleotide array analysis. *Haematologica*, 92, 619–626.

Coyaud, E., Struski, S., Prade, N., Familiades, J., Eichner, R., Quelen, C., Bousquet, M., Mugneret, F., Talmant, P., Pages, M.P., Lefebvre, C., Penther, D., Lippert, E., Nadal, N., Taviaux, S., Poppe, B., Luquet, I., Baranger, L., Eclache, V., Radford, I., Barin, C., Mozziconacci, M.J., Lafage-Pochitaloff, M., Antoine-Poirel, H., Charrin, C., Perot, C., Terre, C., Brousset, P., Dastugue, N. & Broccardo, C. (2010) Wide diversity of PAX5 alterations in B-ALL: a Groupe Francophone de Cytogenetique Hematologique Study. *Blood*, 115, 3089–3097.

DeAngelo, D.J., Hochberg, E.P., Alyea, E.P., Longtine, J., Lee, S., Galinsky, I., Parekkedon, B., Ritz, J., Antin, J.H., Stone, R.M. & Soiffer, R.J. (2004) Extended follow-up of patients treated with imatinib mesylate (gleevec) for chronic myelogeneous leukemia relapse after allogeneic transplantation: durable cytogenetic remission and conversion to complete donor chimerism without graft-versus-host disease. *Clinical Cancer Research*, 10, 5065–5071.

Ellisen, L.W., Bird, J., West, D.C., Soreng, A.L., Reynolds, T.C., Smith, S.D. & Sklar, J. (1991) TAN-1, the human homolog of the Drosophila notch gene, is broken by chromosomal translocations in T lymphoblastic neoplasms. *Cell*, 66, 649–661.

Gedman, A.L., Chen, Q., Kugel Desmoulin, S., Ge, Y., Lafiura, K., Haska, C.L., Cherian, C., Devidas, M., Linda, S.B., Taub, J.W. & Matherly, L.H. (2009) The impact of NOTCH1, FBW7 and PTEN mutations on prognosis and downstream signaling in paediatric T-cell acute lymphoblastic leukemia: a report from the Children's Oncology Group. *Leukemia*, 23, 1417–1425.

Graux, C., Stevens-Kroef, M., Lafage, M., Dastugue, N., Harrison, C.J., Mugneret, F., Bahloula, K., Struski, S., Gregoire, M.J., Nadal, N., Lippert, E., Taviaux, S., Simons, A., Kuiper, R.P., Moorman, A.V., Barber, K., Bosly, A., Michaux, L., Vandenberghe, P., Lahortiga, I., de Keersmaecker, K., Wlodarska, I., Cools, J., Hagemeijer, A. & Poirel, H.A. (2009) Heterogeneous patterns of amplification of the NUP214-ABL1 fusion gene in T-cell acute lymphoblastic leukemia. *Leukemia*, 23, 125–133.

van Grotel, M., Meijerink, J.P., Beverloo, H.B., Langerak, A.W., Buys- Gladdines, J.G., Schneider, P., Poulsen, T.S., den Boer, M.L., Horstmann, M., Kamps, W.A., Veerman, A.J., van Wering, E.R., van Noesel, M.M. & Pieters, R. (2006) The outcome of molecularcytogenetic subgroups in pediatric T-cell acute lymphoblastic leukemia: a retrospective study of patients treated according to DCOG or COALL protocols. *Haematologica*, 91, 1212–1221.

Hagemeijer, A. & Graux, C. (2010) ABL1 rearrangements in T-cell acute lymphoblastic leukemia. *Genes, Chromsomes & Cancer*, 59, 299.

Hammond, D.W., Goepel, J.R., Aitken, M., Hancock, B.W., Potter, A.M. & Goyns, M.H. (1992) Cytogenetic analysis of a United Kingdom series of non-Hodgkins lymphomas. *Cancer Genetics and Cytogenetics*, 61, 31–38.

Heerema, N.A., Sather, H.N., Sensel, M.G., Kraft, P., Nachman, J.B., Steinherz, P.G., Lange, B.J., Hutchinson, R.S., Reaman, G.H., Trigg, M.E., Arthur, D.C., Gaynon, P.S. & Uckun, F.M. (1998) Frequency and clinical significance of cytogenetic abnormalities in pediatric T-lineage acute lymphoblastic leukemia: a report from the Children's Cancer Group. *Journal of Clinical Oncology*, 16, 1270–1278.

Horsman, D.E., Connors, J.M., Pantzar, T. & Gascoyne, R.D. (2001) Analysis of secondary chromosomal alterations in 165 cases of follicular lymphoma with t(14;18). *Genes, Chromosomes and Cancer*, 30, 375–382.

Kaneko, Y., Frizzera, G., Maseki, N., Sakurai, M., Komada, Y., Hiyoshi, Y., Nakadate, H. & Takeda, T. (1988) A novel translocation, t(9;17)(q34;q23), in aggressive childhood lymphoblastic lymphoma. *Leukemia*, 2, 745–748.

von Lindern, M., Breems, D., van Baal, S., Adriaansen, H. & Grosveld, G. (1992) Characterization of the translocation breakpoint sequences of two DEK-CAN fusion genes present in t(6;9) acute myeloid leukaemia and a SET-CAN fusion gene found in a case of acute undifferentiated leukemia. *Genes, Chromosomes and Cancer*, 5, 227–234.

Lones, M.A., Heerema, N.A., Le Beau, M.M., Sposto, R., Perkins, S.L., Kadin, M.E., Kjeldsberg, C.R., Meadows, A., Siegel, S., Buckley, J., Abromowitch, M., Kersey, J., Bergeron, S., Cairo, M.S. & Sanger, W.G. (2007) Chromosome abnormalities in advanced stage lymphoblastic lymphoma of children and adolescents: a report from CCG-E08. *Cancer Genetics and Cytogenetics*, 172, 1–11.

Malyukova, A., Dohda, T., von der Lehr, N., Akhoondi, S., Corcoran, M., Heyman, M., Spruck, C., Grander, D., Lendahl, U. & Sangfelt, O. (2007) The tumor suppressor gene hCDC4 is frequently mutated in human T-cell acute lymphoblastic leukemia with functional consequences for Notch signaling. *Cancer Research*, 67, 5611–5616.

Michaux, L., Wlodarska, I., Rack, K., Stul, M., Criel, A., Maerevoet, M., Marichal, S., Demuynck, H., Mineur, P., Kargar Samani, K., Van Hoof, A., Ferrant, A., Marynen, P. & Hagemeijer, A. (2005) Translocation t(1;6)(p35.3;p25.2): a new recurrent aberration in "unmutated" B-CLL. *Leukemia*, 19, 77–82.

Mrózek, K., Prior, T.W., Edwards, C., Marcucci, G., Carroll, A.J., Snyder, P.J., Koduru, P.R.K., Theil, K.S., Pettenati, M.J., Archer, K.J., Caligiuri, M.A., Vardiman, J.W., Kolitz, J.E., Larson, R.A. & Bloomfield, C.D. (2001) Comparison of cytogenetic and molecular genetic detection of t(8;21)

and inv(16) in a prospective series of adults with de novo acute myeloid leukaemia: a Cancer and leukemia Group B study. *Journal of Clinical Oncology*, **19**, 2482–2492.

Murphy, S. (1980) Classification, staging, and end results of treatment of childhood non-Hodgkin's lymphomas: dissimilarities from lymphomas in adults. *Seminars in Oncology*, **7**, 332–339.

Park, M.J., Taki, T., Oda, M., Watanabe, T., Yumura-Yagi, K., Kobayashi, R., Suzuki, N., Hara, J., Horibe, K. & Hayashi, Y. (2009) FBXW7 and NOTCH1 mutations in childhood T cell acute lymphoblastic leukaemia and T cell non-Hodgkin lymphoma. *British Journal of Haematology*, **145**, 198–206.

Raetz, E.A., Perkins, S.L., Bhojwani, D., Smock, K., Philip, M., Carroll, W.L. & Min, D.J. (2006) Gene expression profiling reveals intrinsic differences between T-cell acute lymphoblastic leukemia and T-cell lymphoblastic lymphoma. *Pediatric Blood and Cancer*, **47**, 130–140.

Rosati, R., La Starza, R., Barba, G., Gorello, P., Pierini, V., Matteucci, C., Roti, G., Crescenzi, B., Aloisi, T., Aversa, F., Martelli, M.F. & Mecucci, C. (2007) Cryptic chromosome 9q34 deletion generates TAF-Iα/CAN and TAF-Iβ/CAN fusion transcripts in acute myeloid leukemia. *Haematologica*, **92**, 232–235.

Sanger, W.G., Armitage, J.O., Bridge, J., Weisenburger, D.D., Fordyce, R. & Purtilo, D.T. (1987) Initial and subsequent cytogenetic studies in malignant lymphoma. *Cancer*, **60**, 3014–3019.

Schneider, N.R., Carroll, A.J., Shuster, J.J., Pullen, D.J., Link, M.P., Borowitz, M.J., Camitta, B.M., Katz, J.A. & Amylon, M.D. (2000) New recurring cytogenetic abnormalities and association of blast cell karyotypes with prognosis in childhood T-cell acute lymphoblastic leukemia: a pediatric oncology group report of 343 cases. *Blood*, **96**, 2543–2549.

Shaffer, L.G. & Tommerup, N. (2005) *ISCN (2005) an International System for Human Cytogenetic Nomenclature*. S. Karger, Basel.

Shikano, T., Ishikawa, Y., Naito, H., Kobayashi, R., Nakadate, H., Hatae, Y. & Takeda, T. (1992) Cytogenetic characteristics of childhood non-Hodgkin lymphoma. *Cancer*, **70**, 714–719.

Uyttebroeck, A., Vanhentenrijk, V., Hagemeijer, A., Boeckx, N., Renard, M., Wlodarska, I., Vandenberghe, P., Depaepe, P. & de Wolf-Peeters, C. (2007) Is there a difference in childhood T-cell acute lymphoblastic leukemia and T-cell lymphoblastic lymphoma? *Leukemia & Lymphoma*, **48**, 1745–1754.

van Vlierberghe, P., van Grotel, M., Tchinda, J., Lee, C., Beverloo, H.B., van der Spek, P.J., Stubbs, A., Cools, J., Nagata, K., Fornerod, M., Buijs-Gladdines, J., Horstmann, M., van Wering, E.R., Soulier, J., Pieters, R. & Meijerink, J.P. (2008) The recurrent SET-NUP214 fusion as a new HOXA activation mechanism in pediatric T-cell acute lymphoblastic leukemia. *Blood*, **111**, 4668–4680.

Weng, A.P., Ferrando, A.A., Lee, W., Morris, J.P., Silverman, L.B., Sanchez-Irizarry, C., Blacklow, S.C., Look, A.T. & Aster, J.C. (2004) Activating mutations of NOTCH1 in human T cell acute lymphoblastic leukemia. *Science*, **306**, 269–271.

Zhu, Y.M., Zhao, W.L., Fu, J.F., Shi, J.Y., Pan, Q., Hu, J., Gao, X.D., Chen, B., Li, J.M., Xiong, S.M., Gu, L.J., Tang, J.Y., Liang, H., Jiang, H., Xue, Y.Q., Shen, Z.X., Chen, Z. & Chen, S.J. (2006) NOTCH1 mutations in T-cell acute lymphoblastic leukaemia: prognostic significance and implication in multifactorial leukemogenesis. *Clinical Cancer Research*, **12**, 3043–3049.

Generation of induced pluripotent stem cells from primary chronic myelogenous leukemia patient samples

Keiki Kumano,[1,2] Shunya Arai,[1,2] Masataka Hosoi,[1,2] Kazuki Taoka,[1,2] Naoya Takayama,[3,4] Makoto Otsu,[5] Genta Nagae,[6] Koki Ueda,[1,2] Kumi Nakazaki,[1,2] Yasuhiko Kamikubo,[1,2] Koji Eto,[3,4] Hiroyuki Aburatani,[6] Hiromitsu Nakauchi,[3,5] and Mineo Kurokawa[1,2]

[1]Department of Hematology and Oncology, Graduate School of Medicine, University of Tokyo, Tokyo, Japan; [2]Core Research for Evolutional Science and Technology, Japan Science and Technology Agency, Tokyo, Japan; [3]Stem Cell Bank, Center for Stem Cell Biology and Regenerative Medicine, Institute of Medical Science, University of Tokyo, Tokyo, Japan; [4]Center for iPS Cell Research and Application, University of Kyoto, Kyoto, Japan; [5]Division of Stem Cell Therapy, Center for Stem Cell Biology and Regenerative Medicine, Institute of Medical Science, University of Tokyo, Tokyo, Japan; and [6]Genome Science Division, Research Center for Advanced Science and Technology, University of Tokyo, Tokyo, Japan

Induced pluripotent stem cells (iPSCs) can be generated by the expression of defined transcription factors not only from normal tissue, but also from malignant cells. Cancer-derived iPSCs are expected to provide a novel experimental opportunity to establish the disease model. We generated iPSCs from imatinib-sensitive chronic myelogenous leukemia (CML) patient samples. Remarkably, the CML-iPSCs were resistant to imatinib although they consistently expressed BCR-ABL oncoprotein. In CML-iPSCs, the phosphorylation of ERK1/2, AKT, and JNK, which are essential for the maintenance of both BCR-ABL (+) leukemia cells and iPSCs, were unchanged after imatinib treatment, whereas the phosphorylation of signal transducer and activator of transcription (STAT)5 and CRKL was significantly decreased. These results suggest that the signaling for iPSCs maintenance compensates for the inhibition of BCR-ABL. CML-iPSC–derived hematopoietic cells recovered the sensitivity to imatinib although $CD34^+38^-90^+45^+$ immature cells were resistant to imatinib, which recapitulated the pathophysiologic feature of the initial CML. CML-iPSCs provide us with a novel platform to investigate CML pathogenesis on the basis of patient-derived samples. (*Blood*. 2012;119(26):6234-6242)

Introduction

Hematologic malignancies including leukemias are often chemotherapy-resistant, most of which follows an aggressive clinical course.[1] Multiple drug therapies are usually required to treat them, although they are occasionally accompanied with many side effects. Thus, the invention of novel targeted therapies based on newly revealed molecular pathogenesis is expected to overcome the current situation.[2] However, previous approaches to understanding pathogenesis involve several limitations. Many mouse models of human diseases have been established, but they may not fully recapitulate many aspects of original human diseases.[3] Many kinds of cell lines are also available for research. However, they do not cover all diseases, because it is usually difficult to establish a cell line from a primary patient sample. Furthermore, additional gene mutations may be accumulated in cell lines. Theoretically, primary patient samples should be used for research, but the amount of obtained cells may be inadequate for various analyses.

Induced pluripotent stem cells (iPSCs) can be generated from various types of cells by the transduction of defined transcription factors.[4-10] In addition to the regenerative medicine,[11] iPSCs have been used for studies of the pathogenesis of inherited genetic diseases.[12-16] Recently, it was reported that iPSCs were generated not only from normal tissue cells, but also from malignant cells.[17-20] In those cases, cancer cells themselves must have been the origins of iPSCs. However, in most published data, established cell lines were used as the source material of cancer cells, including chronic myelogenous leukemia (CML),[17] gastrointestinal cancers,[18] and melanoma,[19] except for the JAK2-V617F mutation (+) polycythemia vera (PV) patient.[20]

CML is a myeloproliferative neoplasm that originates from hematopoietic stem cells transformed by the *BCR-ABL* fusion gene. The initial indolent chronic phase (CP) is followed by aggressive stages, the accelerated phase (AP), and the blast crisis (BC), in which immature leukemic cells expand.[21] CML is now initially treated with one of several tyrosine kinase inhibitors (TKIs) including imatinib, dasatinib, and nilotinib, which have dramatically improved the long-term survival rate of CML patients up to approximately 90%. However, even TKIs are not able to eradicate the CML clone completely, which is demonstrated by the fact that discontinuation of TKIs in molecular remission CML patients usually leads to the recurrence of the BCL-ABL clone. Therefore, many studies are performed to elucidate the mechanisms of TKI-resistance in CML stem cells and to overcome the resistance.

In this study, we established iPSCs from primary CML patient samples, redifferentiated them into hematopoietic lineage and showed the recapitulation of the pathophysiologic features of the initial disease.

Submitted July 14, 2011; accepted April 30, 2012. Prepublished online as *Blood* First Edition paper, May 16, 2012; DOI 10.1182/blood-2011-07-367441.

The online version of this article contains a data supplement.

The publication costs of this article were defrayed in part by page charge payment. Therefore, and solely to indicate this fact, this article is hereby marked "advertisement" in accordance with 18 USC section 1734.

Methods

Cell and cell culture

Primary samples of CML bone marrow cells were obtained after informed consent. All studies using human cells were reviewed and approved by the institutional review boards (IRBs) of University of Tokyo. Mononuclear cells (MNCs) were isolated by centrifugation through a Ficoll gradient. $CD34^+$ cells were isolated by an immunomagnetic separation technique (auto magnetic-activated cell sorting; MACS). They were cultured with α-minimum essential medium (MEM) containing 20% fetal calf serum (FCS) supplemented with 100 ng/mL stem cell factor (SCF; Wako), 10 ng/mL thrombopoietin (TPO; Wako), 100 ng/mL FL3L (Wako), 10 ng/mL IL3 (Wako), and 100 ng/mL IL6 (Wako).

Normal iPSCs established from cord blood (CB) $CD34^+$ cells or fibroblasts[22] and CML-iPSCs were maintained in Dulbecco modified Eagle medium-F12 (Invitrogen) supplemented with 20% knockout serum replacement (KSR; Invitrogen), 0.1mM 2-mercaptoethanol (Sigma-Aldrich), MEM nonessential amino acids (Invitrogen), and 5 ng/mL recombinant human basic fibroblast growth factor (FGF; Peprotech) on mitomycin C (MMC)–treated mouse embryo fibroblast (MEF) feeder cells.[23] Imatinib (LC Laboratories) was added to the culture medium at the various concentrations (1-10μM). U0126 and LY294004 (LC Laboratories) were used to inhibit ERK and AKT, respectively.

The mouse C3H10T1/2 cells were cultured as previously described.[24]

Production of VSV-G pseudotyped retroviral particles

Construction of pMXs vectors encoding Oct3/4, Sox2, Klf4, and c-myc were performed as previously described.[22] Highly concentrated VSV-G–pseudotyped retroviral supernatant was prepared using reported procedures. The 293GPG cells were kind gifts from Dr R. C. Mulligan (Children's Hospital Boston, Harvard Medical School, Boston, MA).[25] Stable 293GPG cell lines, each capable of producing VSV-G–pseudotyped retroviral particles on induction were established as previously described.[22,25] Retroviral supernatants were concentrated by centrifugation for 16 hours at 6000*g*.

Generation of iPSCs from CML samples

Two days before infection, cells were stimulated with cytokines as mentioned in "Cell and cell culture." For infection, each well of a 24-well dish coated with a fibronectin fragment CH296:RetroNectin (Takara-Bio) was covered with virus-containing supernatants. After the adhesion of viruses according to the manufacture's recommendation, 1×10^5 cells of $CD34^+$ CML cells or CB cells were inoculated into each well and filled with the culture medium supplemented with cytokines. The next day, concentrated viral supernatant was added to the culture. On day 3 after infection, cells were harvested with vigorous pipetting, washed by phosphate-buffered saline (PBS), and cultured with the same fresh medium for next 3 days. On day 6, cells were seeded on MMC treated MEF cells. Two to 4 days after, the medium was replaced with human ES medium as previously described with 0.5mM valproic acid (VPA; Sigma-Aldrich).[26] Subsequently, medium was changed every other day. After 20 days, ES-like colonies appeared. Using live cell imaging technology with Tra-1-60 antibody as previously described,[27] each fully reprogrammed colony was distinguished from deficiently reprogrammed colonies, and was picked up to be reseeded on new MEF feeder cells. Cloned ES-like colonies were subjected to further analysis.

Antibodies, FACS analysis, and immunocytochemistry

The following fluorescent conjugated antibodies were used for fluorescence-activated cell sorter (FACS) analysis and immunocytochemistry: anti–human stage specific embryonic antigen (SSEA)–4 conjugated with Alexa Fluor 488 (BD Bioscience), anti–human tumor related antigen (TRA)–1-60 conjugated with Alexa Fluor 555 (BD Bioscience), anti-CD34 phycoerythrin (PE) conjugated (Beckman Coulter), and anti-CD45 fluorescein isothiocyanate (FITC) conjugated (Beckman Coulter).

Cells were sorted with a FACSAria, and analysis was performed on FACS LSRII (BD Bioscience).

For immunocytochemistry, cells were fixed with 4% paraformaldehyde in PBS, after which they were labeled with an antibody against human SSEA-4 and antibody against human TRA-1-60 antibody and observed using a confocal microscope (Carl Zeiss).

Methylation profiling

Genomic DNA was extracted using the QIAamp DNA Mini Kit (QIAGEN) according to the manufacture's instruction. Methylation status was evaluated as previously reported.[28] Methylation status was analyzed using HumanMethylation27 BeadChip (Illumina). Genomic DNA for methylation profiling was quantified using the Quant-iT dsDNA BR assay kit (Invitrogen). Five-hundred nanograms of genomic DNA was bisulfite-converted using an EZ DNA methylation kit (Zymo Research). The converted DNA was amplified, fragmented and hybridized to a beadchip according to the manufacturer's instructions. The raw signal intensity for both methylated (M) and unmethylated (U) DNA was measured using a BeadArray Scanner (Illumina). The methylation level of the each individual CpG is obtained using the formula (M)/(M) + (U) + 100 by the GenomeStudio (Illumina).

Microarray analysis

Gene expression analysis was carried out as previously described[29] with the use of the Human Genome U133 Plus 2.0 Array (Affymetrix). The hierarchical clustering techniques classify data by similarity and their results are represented by dendrograms. Previously reported data of human embryonic stem (ES) cells (GSM449729) and CML $CD34^+$ cells (GSM366215, 366216, 366221, and 366222) were used to compare the gene expression profile. The microarray data are available on the Gene Expression Omnibus (GEO) database under accession number GSE37982.

Hematopoietic differentiation of iPSCs

To differentiate iPSCs into hematopoietic cells, we used the same protocol previously used with ES cells and iPSCs.[22,24] In brief, small clusters of iPSCs (< 100 cells treated with PBS containing 0.25% trypsin, 1mM $CaCl_2$, and 20% KSR) were transferred onto irradiated 10T1/2 cells and cocultured in hematopoietic cell differentiation medium, which was refreshed every third day. Differentiation medium consists of Iscove modified Dulbecco medium supplemented with a cocktail of 10 μg/mL human insulin, 5.5 μg/mL human transferrin, 5 ng/mL sodium selenite, 2mM L-glutamine, 0.45mM α-monothioglycerol, 50 μg/mL ascorbic acid, and 15% highly filtered FBS in the presence of 20 ng/mL human vascular endothelial growth factor (VEGF).[24] On days 14 to 15 of culture, the iPS-sacs were collected into a 50-mL tube, gently crushed with a pipette tip and passed through a 40-μm cell strainer to obtain hematopoietic progenitors. Hematopoietic progenitors were collected by sorting with CD34 and CD45 antibodies, Giemsa stained, and then examied under a microscope. Hematopoietic progenitors were cultured in the α-medium plus 20% FCS supplemented with 100 ng/mL SCF, 10 ng/mL TPO, 100 ng/mL FL3L, 10 ng/mL IL3, and 100 ng/mL IL6.

Hematopoietic colony-forming cell (CFC) assay

CFC assays were performed in MethoCult H4434 semisolid medium (StemCell Technologies). Ten thousand hematopoietic progenitors harvested from an iPS-Sacs were plated in 1.5 mL of medium and cultivated for 14 days.

RT-PCR and quantitative real-time PCR analysis

After extraction of total RNA with RNAeasy reagents (QIAGEN), reverse transcription was performed with SuperScript III (Invitrogen). Primer

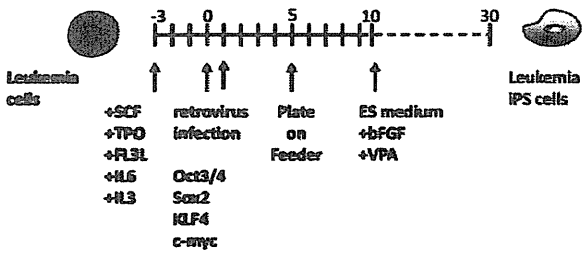

Figure 1. Experimental scheme for generating of iPSCs from the CML patient sample. After cytokine stimulation, $CD34^+$ CML cells were reprogrammed by transduction with Yamanaka factors. To improve the reprogramming, valproic acid was added to the culture.

sequences used for the detection of stem cell genes were as previously described.[9]

Quantitative real-time PCRs (qPCRs) were carried out in the ABI-7000 sequence detection system with SYBR Green PCR Core reagents according to the manufacturer's instructions (Applied Biosystems). We analyzed expression levels of *BCR-ABL* fusion transcript as previously described.[30] Each assay was performed in triplicate and the results were normalized to GAPDH (glyceraldehyde-3-phosphate dehydrogenase) levels.

PCR primers used for quantitative PCR:
BCR-ABL F TCAGAAGCTTCTCCCTGACATCCGT
BCR-ABL R TCCACTGGCCACAAAATCATACAGT
GAPDH F TGCACCACCAACTGCTTAGC
GAPDH R GGCATGGACTGTGGTCATGAG

Western blotting

Fifty micrograms of cell lysates were subjected to sodium dodecylsulfate-polyacrylamide gel electrophoresis (SDS-PAGE) and Western blot analysis. Antibodies used in immunoblotting were as follows; anti-phospho ERK1/2 (Thr202/Tyr204; Cell Signaling), anti-phospho Akt (Ser473; Cell Signaling), anti-phospho JNK (Thr183/Tyr185; Cell Signaling), anti-phospho-STAT5 (Tyr694; Cell Signaling), and anti-phospho CRKL (Tyr207; Cell Signaling). Enhanced chemiluminescence detection (Amersham) was carried out according to the manufacturer's recommendations.

Results

Generation of iPSCs from primary CML patient samples

After obtaining informed consent, $CD34^+$ cells were purified from bone marrow mononuclear cells of a CML chronic phase patient. After we stimulated them with cytokines for 2 days, retroviral transduction with the transcription factors OCT3/4, SOX2, KLF4, and MYC was performed. Two days after transduction, we reseeded cells onto MEF cells and cultured them for another 2 days. Then, we replaced the medium with human ES medium supplemented with 5 ng/mL bFGF. To improve the efficiency of the reprogramming, we added VPA,[26] a histone deacetylase inhibitor, to the culture (Figure 1). Using a live cell imaging method with Tra-1-60 antibody, bona fide iPSCs were distinguished from deficiently reprogrammed cells.[27] As a result, 2 CML-derived iPSCs (CML-iPSCs) were generated, which were derived from independent patients. CML-iPSCs showed the typical morphology as iPSCs (Figure 2A) and expressed the pluripotency markers, such as SSEA-4 and Tra-1-60 (Figure 2B), and the endogenous expression of embryonic stem cell (ESC) characteristic transcripts (OCT3/4, SOX2, KLF4, NANOG, LIN28, and REX1) was confirmed by RT-PCR (Figure 2C). CML-iPSCs also expressed BCR-ABL, which demonstrated that they were truly derived from CML (Figure 2D). Furthermore, fluorescence in situ hybridization with dual color *BCR-ABL* probes confirmed t(9;22) translocation in CML-iPSCs at the single cell level (supplemental Figure 1A and supplemental Table 1, available on the *Blood* Web site; see the Supplemental Materials link at the top of the online article). However, although CML-iPSCs expressed BCR-ABL, they were resistant to imatinib (Figure 2E). Teratoma formation capacity was confirmed, demonstrating the pluripotency of CML-iPSCs (supplemental Figure 2).

Comprehensive analysis of DNA methylation revealed that methylation pattern of CML-iPSCs was different from that of original CML sample but was very similar to that of normal iPSCs although there were slight differences (Figure 3A). Previously, stem cell–specific differentially methylated regions (SS DMRs)

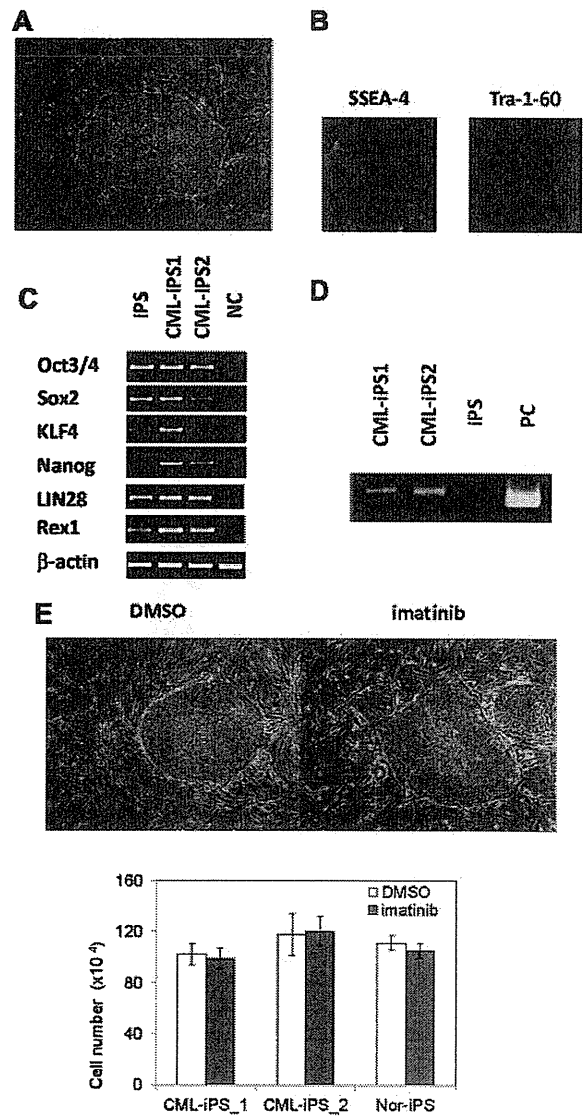

Figure 2. Generation of CML derived iPSCs. (A) Morphology of CML-iPSCs. (B) Immunofluirescence staining shows expression of pluripotent marker (left: SSEA-4 and right: Tra-1-60) in CML-iPSCs. (C) RT-PCR analysis of ES cell marker genes. Endogenous expression of these stem cell–specific genes in CML-iPSCs was verified. (D) CML-iPSCs expressed the BCR-ABL fusion transcript. (E) Imatinib (10μM) were added to the culture of iPSCs. DMSO (top left panel) and imatinib (top right panel) treated CML-iPSCs were shown. The number of alive CML-iPSCs (CML-iPS_1 and CML-iPS_2) and normal iPSCs (Nor-iPS) after 5 days treatment was calculated (bottom panel). These were the representative data from 3 independent experiments.

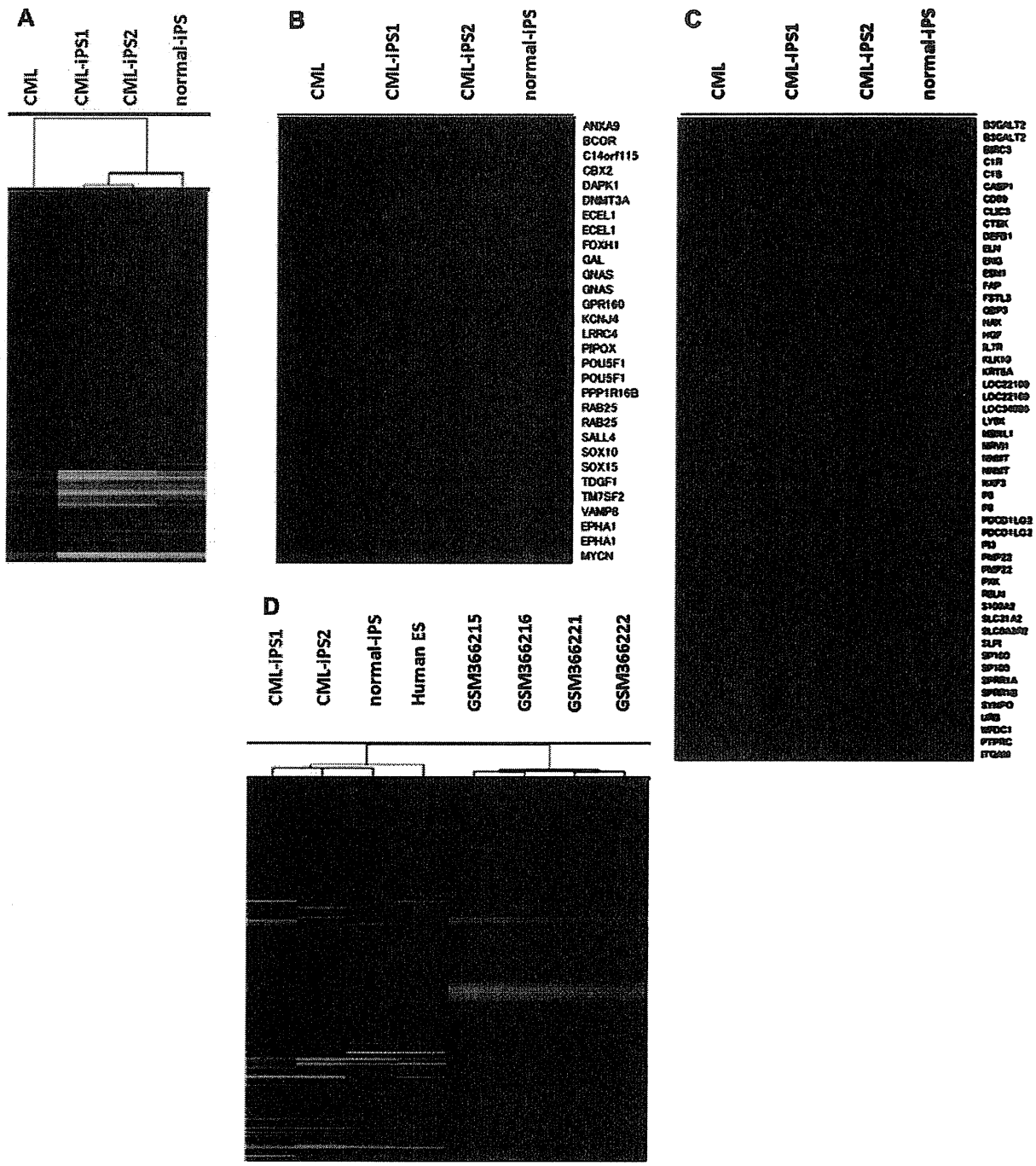

Figure 3. Comprehensive analysis of DNA methylation and gene expression. (A) Unsupervised hierarchical clustering based on differentially methylated CpGs is shown on the dendrogram. The accompanying heatmap shows the methylation status across 5001 differentially methylated CpGs. In the heatmap, red indicates a CpG methylation more than 50%, and green less than 50%. The methylation status in hypo SS DMRs (B) or hyper SS DMRs (C) was shown in the heatmap. (D) Unsupervised hierarchical clustering based on global gene expression data are shown on the dendrogram. The accompanying heatmap shows the normalized log2 transformed expression values (Z-scores) for each probe. In the heatmap, red indicates expression more than mean, and green less than mean.

were identified during reprogramming process of iPSCs.[31] Hypomethylated SS DMRs (hypo SS DMRs) in the variety of iPSCs were also hypomethylated in the CML-iPSCs including the promoters of OCT4 (Figure 3B). In the same way, hypermethylated SS DMRs (hyper SS DMRs) in the variety of iPSCs were also hypermethylated in the CML-iPSCs (Figure 3C). The promoters of hematopoietic lineage-specific marker genes, such as CD45 and CD11b, were hypermethylated in the CML-iPSCs. Thus, the methylation pattern of CML-iPSCs was confirmed to be not hematopoietic cell-like, but iPSC-like. Next, we compared the gene expression pattern among CML-iPSCs and normal iPSCs (Figure 3D). In a result, CML-iPSCs and normal iPSCs were very similar in regard to global gene expression profile. Furthermore, comparing our results with publicly available expression data of human ES cells and CML $CD34^+$ cells, we found that CML-iPSCs were very similar to human ES cells, whereas they were different